DUST DRIVEN WINDS

Erwin Sedlmayr and Carsten Dominik*
Institut für Astronomie und Astrophysik, Technische Universität Berlin, Hardenbergstr. 36, D-10623 Berlin, Germany

March 4, 1994

Abstract. The status of dust driven winds, constituting an important subclass of essentially radiation generated winds, is surveyed. Dust driven winds are conceived as a long lasting phenomenon of heavy mass loss concerning those luminous cool giants and supergiants, where dust condensation in the expanding flow determines both the *stellar mass loss rate* and the *subsonic–supersonic transition* of the velocity field. Our contribution aims at a selfconsistent description of the dynamical shell structure with particular emphasis to the theoretical aspects of this important phenomenon. Thus, not only the complex coupling of the various ingredients (hydrodynamics, chemistry, radiative transfer, dust nucleation and growth) is outlined in detail, but also general arguments regarding the overall structure of such winds and the expected position of their central objects in the Hertzsprung-Russel diagram are conducted. A selected typical selfconsistent model for a stationary C-star shell demonstrates the characteristic wind structure and gives insight into the close nonlinear interplay between dust formation and wind generation. During the late evolutionary stages of a star along the AGB dust driven mass loss provides a natural self–accelerating mechanism which easily can produce very high mass loss rates, an effect which possibly might play an important role for the Tip-AGB objects and the AGB-PN-transition.

Contents

* Present Address: NASA Ames Research Center, Mail Stop 245–3, Moffett Field, CA 94035–1000, USA

1 Introduction

Stellar winds are a common phenomenon which is observed at nearly all stages of main sequence and post main sequence evolution, thus causing a continuous mass loss during most of the active life time of a star. For the sun, the present mass loss rate $\dot{M} = 2 \cdot 10^{-14} M_{\odot} \mathrm{yr}^{-1}$ is very small, but for very luminous red giants and supergiants $\dot{M}$ can amount to tremendously high values up to $10^{-4} M_{\odot} \mathrm{yr}^{-1}$.

Inspection of the Hertzsprung-Russell-diagram shows that significant mass loss rates (say $\dot{M} > 10^{-6} M_{\odot} \mathrm{yr}^{-1}$) caused by winds only are to be expected for high luminosity objects like massive hot stars at the upper region of the main sequence (in this context see the review of [Kudritzki *et al.* 1991]) or low mass cool giants and supergiants with effective temperatures T_* below 3500 K (e.g. [deJager 1983] [deJager *et al.* 1988] and [Lafon and Berruyer 1991]).
These investigations indicate that nearly 90% of the total stellar mass loss in our galaxy originates from *cool high luminosity stars*, i.e. red giants and supergiants, in particular from Asymptotic Giant Branch (AGB) stars, which by far provide the largest contribution to the stellar mass injection rate into the interstellar medium (cf. [Gehrz 1989]). Since the outflows of these stars usually show considerable fractions of circumstellar dust, a close connection between dust condensation and the dynamical wind structure is naturally suggested (cf. [Sedlmayr 1994]).

Regarding the driving mechanism for a stellar wind, basically two possibilities are distinguished:

- radiation driven winds
- pressure driven winds.

In the case of *radiation driven winds*, the acceleration of the matter is caused by the *absorption of radiative momentum* in the outermost layers of the stellar atmosphere by either the plasma components (winds of *hot* stars) or by molecules and dust particles (winds of *cool* stars). In the case of *pressure driven winds*, the acceleration is attributed to the *dissipation of mechanical energy* provided by convection zones, stellar pulsations, shock waves etc. at some outer region of the star's atmosphere. Examples for pressure driven winds are the solar wind, which is generated by the dissipation of mechanical energy originating from the solar convection zone, and winds of pulsating variables which are induced by shock wave dissipation in the extended shells.

In many situations, however, the above distinction between radiation driven and pressure driven winds is not always as clear. During the late evolutionary stages, most cool stars undergo more or less pronounced non-stationary phases where a mutual support of mechanical and radiative forces for the wind generation is to be expected. Usually this process is considered as a two step process:

– levitation of the atmosphere by mechanical energy and/or radiation pressure on molecules, and subsequent

– acceleration of the matter by radiation pressure, especially on dust grains.

Regarding the wind generation of cool stars, in particular three different cases are discussed in this context:

a) Levitation of a hydrostatic atmosphere by *radiation pressure on molecular lines* [Jørgensen and Johnson 1992]. In this way, the cool outer layers of a red giant are shifted outwards causing the pressure scale height to be considerably increased. For very high luminous stars, the radiative momentum input can be sufficient for the extended atmosphere to surmount the escape point resulting in a continuous stationary mass loss.

b) Levitation of a hydrostatic atmosphere by *mechanical momentum and energy input due to waves* (e.g. acoustic waves, Alfvén waves, etc.). Corresponding mechanisms which have been proposed e.g. by [Pijpers and Hearn 1989] and [Hartmann and MacGregor 1980], also cause a considerable extension of the atmosphere which may be sufficient for generating a pronounced stellar mass loss (cf. [Pijpers and Habing 1989], [Hearn 1990]).

In both cases a) and b), the levitation of matter favours improved conditions for dust nucleation and grain growth causing a dust shell to develop. If dust particles are present, a very effective momentum transfer from the radiation field to the gas by photon absorption of the grains and by their frictional coupling to the gas is induced which then determines the local velocity field causing a steep acceleration zone. For judging the role of the dust component for the wind generation, two cases with regard to grain formation have to be distinguished:

i) Grain formation, and hence the steep velocity increase, takes place *outside the sonic point* of the monotonic velocity field. In these cases, dust formation causes only a more or less dramatic increase of the expansion velocity but *cannot* influence the mass loss rate $\dot{M}$ of the star, which is solely given by the inner levitation mechanism.

ii) Grain formation takes place *inside the sonic point*. In these cases, dust formation determines both the *subsonic-supersonic transition* of the velocity field *and* the *mass loss rate* $\dot{M}$ of the star, irrespective of the basic levitation mechanism inside. It is basically this situation where the mass loss rate is determined by the dust formation process which is addressed as a *dust driven wind*.

Hitherto no satisfactory quantitative description of the mechanical energy and momentum input for stationary levitation is available and the approaches applied (e.g. [Holzer and MacGregor 1985], [Pijpers and Habing 1989] and [Hearn 1990]) adopt a parameterized incorporation of the mechanical acceleration terms, which allow to exhibit the basic dynamical effects but are far from providing a selfconsistent model of the local energy and momentum transfer. For this reason, we confine our discussion to the important subclass of *dust driven winds* which are purely radiation generated. In this case, the selfconsistent wind models are completely determined by the specification of four independent fundamental stellar parameters: e.g. mass M_*, luminosity L_*, effective temperature T_*, and chemical abundances $\{\epsilon_\ell\}$, where ℓ numbers the relevant chemical elements. All other quantities, in particular the mass loss rate $\dot{M}$, are then uniquely provided by the selfconsistent model ([Gail and Sedlmayr 1987b]).

c) Generation of the mass loss by *shock waves* originating from stellar pulsations inside which run through the extended dynamical atmosphere and push the matter outwards (e.g. [Bowen 1988a; Bowen 1988b], [Bowen 1990], [Bowen and Willson 1991]). By this effect, a characteristic radial structure with regard to the density and the temperature is induced in the shell allowing for effective dust condensation in rather narrow regions behind the shock fronts ([Fleischer *et al.* 1992]). These pronounced onion-like dust shells then are effectively accelerated by radiation pressure causing a steep increase of both the velocity field and the mass loss rate. By this complex interplay of hydrodynamics and dust condensation, the observed high mass loss rates of Miras and LPVs and their optical appearance can be consistently explained ([Fleischer 1994], [Winters *et al.* 1993; Winters 1994]).

   An important result of these investigations is that even in the limit of vanishing mechanical momentum and energy input, selfconsistent wind solutions in the high luminosity domain exist, which in case of negligible dust backwarming are identical to the stationary ab initio models of case a) being completely determined by the four fundamental stellar parameters M_*, L_*, T_* and $\{\epsilon_\ell\}$ ([Fleischer 1994]). This behaviour gives confidence in the above definitions of stationary dust driven winds and supports the assumption that these objects form an important sub-class consisting of high luminosity cool giants and supergiants showing very large mass loss rates.

Although the idea of dust driven mass loss has been put forward by many papers in the past, it was not before the last decade that a realistic description of this important phenomenon has been achieved and selfconsistent models are available ([Gail and Sedlmayr 1987b]). The reason for this is that the reliable description of a dust driven wind requires the simultaneous treatment of four closely coupled nonlinear problems:

- thermodynamic and hydrodynamic structure of the shell

- radiative transfer

– chemical structure of the shell

– dust condensation and growth.

Especially the last two complexes (chemistry and dust formation), which are of fundamental importance for a quantitative understanding of a dust driven wind, require a detailed discussion of the relevant molecules and a reliable description of the gas–solid phase transition.

In the subsequent chapters, the observational situation regarding those objects which are expected to have dust driven winds is stated and a consistent theoretical description of this phenomenon is conducted.

2 Observations of circumstellar dust shells

In the last two decades, a tremendous amount of observational material has been compiled in nearly every spectral regime to explore the detailed appearance of evolved stellar objects, their evolutionary status, and the basic mechanisms determining their dynamics. For this reason, we do not feel prepared to present a complete adequate survey of the existing observational work, but instead refer to few relevant reviews and some sort of key papers and references therein. Moreover, as this review essentially is concerned with theoretical aspects, we confine our scope to papers having a direct impact on our subject.

The objects under consideration are intrinsically cool AGB stars ($T_\star < 3000$K), which are surrounded by considerable amounts of dust. Since the dust particles are effective absorbers of radiative energy, which they reradiate at even longer wavelengths after an internal relaxation process, dusty AGB stars are primarily infrared sources.

Improved instrumental capabilities in the long wavelength spectral range have led to an increased interest in observations of late–type giants in the last years and produced a vast amount of observational data. This provided an extensive basis for a more thorough understanding of these objects. Based on this material e.g. [Sopka *et al.* 1985], [Claussen *et al.* 1987], [Thronson *et al.* 1987], [Willems and deJong 1988], [Jura *et al.* 1989], [Jura and Kleinmann 1989], [Groenewegen *et al.* 1992] were able to derive e.g. mass loss rates, gas–to–dust ratios, distances, luminosities and final outflow velocities for various large samples of objects.

In a recent extensive catalogue of CO and HCN observations, [Loup *et al.* 1993] compile values of the mass loss rate and the terminal wind velocity for a sample of 444 circumstellar envelopes. This catalogue includes the values published in the original literature between January 1985 and September 1992. The sample contains 184 oxygen–rich, 205 carbon–rich, and 9 S–stars. About 85% of the sources are AGB stars, 32 are planetary nebulae and about thirty are post–AGB star candidates. These objects cover a range in mass loss rate of $10^{-8} \lesssim \dot{M} \lesssim$

$10^{-4} M_{\odot} \mathrm{yr}^{-1}$ and a range in terminal velocity of $3\,\mathrm{kms}^{-1} < v_{\infty} \lesssim 40\,\mathrm{kms}^{-1}$. Most of the oxygen–rich sources (86%) have $5\,\mathrm{kms}^{-1} < v_{\infty} < 20\,\mathrm{kms}^{-1}$ with a peak of the distribution between 10 and $20\,\mathrm{kms}^{-1}$ while 92% of the C–stars have v_{∞} between 5 and $30\,\mathrm{kms}^{-1}$ and the peak of the distribution occurs between 10 and $15\,\mathrm{kms}^{-1}$. For M–stars, the velocity distribution drops drastically for $v_{\infty} > 20\,\mathrm{kms}^{-1}$ while it is quite continuous for C–stars up to $v_{\infty} \approx 35\,\mathrm{kms}^{-1}$. Typically, the M–stars have mass loss rates in the range between 10^{-7} and $5 \cdot 10^{-5} M_{\odot} \mathrm{yr}^{-1}$ and the C–stars have $3 \cdot 10^{-7} < \dot{M} < 5 \cdot 10^{-5} M_{\odot} \mathrm{yr}^{-1}$ and tend to show on average the higher values than the oxygen–rich AGB objects.

Up to now, the most accurate determination of mass loss rates and final outflow velocities is obtained by high resolution observations in the radio spectral range. The observed widths of the molecular rotation lines (mainly of CO) provide rather reliable values of the expansion velocities of the circumstellar shells (e.g. [Knapp *et al.* 1982; Knapp and Morris 1985; Knapp 1987]). By calculating theoretical profiles of the CO J=1–0 and J=2–1 rotational lines, [Knapp and Morris 1985] derived mass loss rates for 50 late–type M and C–stars in the range from $\sim 10^{-7}$ up to some $10^{-4} \mathrm{M}_{\odot} \mathrm{yr}^{-1}$. Although this is the most accurate method applied so far, the values of the mass loss rates as derived from molecular rotation line observations generally are uncertain by a factor of $2 - 3$ (cf. [Knapp and Morris 1985; Knapp 1987; Veen and Rugers 1989]), besides the error introduced by the often poorly known distances to the objects.

Applying radiative transfer models for fitting the observed infrared fluxes, dust mass loss rates may be derived if the outflow velocity is known. Comparing the values resulting from this method with the gas mass loss rates derived from molecular line observations, it is found, that the gas loss rates are proportional to the dust loss rates over the entire range of mass loss rates ($10^{-7} \lesssim \dot{M} \lesssim 10^{-4} M_{\odot} yr^{-1}$, e.g. [Sopka *et al.* 1985], [Knapp 1985], [Jura 1986a]).

Applying both methods, values of the dust to gas ratio can be obtained, which for carbon–rich CDS typically are $\rho_d/\rho_g \approx 2 \ldots 3 \cdot 10^{-3}$ and for oxygen–rich envelopes $\rho_d/\rho_g \approx 6 \ldots 6.6 \cdot 10^{-3}$ ([Knapp 1985]) over a wide range of mass loss rates, i.e. this ratio is fairly constant for all carbon–rich and oxygen–rich circumstellar shells. Since the constancy of this ratio is a necessary condition for an outflow caused by radiation pressure on dust with subsequent momentum transfer to the gas, the observed correlation strongly supports the hypothesis, that the winds of these objects are in fact dust driven.

From CO(J=1–0), HCN(J=1–0), $\mathrm{HC_3N}$(J=10–9), and HNC(J=1–0) emission line observations of 23 well known evolved stars [Sopka *et al.* 1989] derive mass loss rates ($1 \cdot 10^{-6} < \dot{M} < 1.4 \cdot 10^{-4} M_{\odot} \mathrm{yr}^{-1}$), envelope sizes ($3 \cdot 10^{15}\mathrm{cm} < R_{\mathrm{Env}} < 3 \cdot 10^{18}\mathrm{cm}$), molecular abundances, isotope ratios, and gas–to–dust ratios in the range $1.6 \cdot 10^{-3} \lesssim \rho_d/\rho_g \lesssim 3.6 \cdot 10^{-2}$.

A further finding from the observations is, that dust forming cool giants generally do not possess chromospheres ([Jura 1986b]). Since interstellar UV photons cannot penetrate into the inner region of the dust shell ([Mamon *et al.* 1988]), photo-reactions can be neglected in the dust formation region (cf. Sects. 4.1 and 4.2).

The suggestion, that radiation pressure on dust grains alone might be sufficient for driving the outflow ([Wickramasinghe *et al.* 1966]) has been further supported by empirical evidence. If radiation pressure on dust grains causes the outflow, then the momentum flux of the radiation field should be related to the momentum flux of the outflowing material. The observations indicate, that in many dust–forming shells the ratio between the momentum flux of the material and the momentum flux of the radiation field is of the order of unity ([Jura 1986a]) and proportional to the UV optical depth of the dust component in the circumstellar shell ([Knapp 1986]). From CO(J=2–1) emission line observations of infrared bright stars [Zuckerman and Dyck 1986] find e.g. for 11 objects $\dot{M}v_\infty\,c/L_\star = 3\ldots 12$, from which 9 objects are carbon–rich. Most of the in total 37 objects however are found to have $\dot{M}v_\infty < L_\star/c$. These results confirm, that radiation pressure on dust grains at least accelerates the wind to its terminal velocity in most of these objects.

Concerning the internal structure of the dust grains actually formed in the circumstellar shells, some information can be gained from the slope of the infrared spectra. Recent spectral modelling ([Jura 1983], [Jura 1986a]; [Sopka *et al.* 1985]; [Martin and Rogers 1987]; [Rose 1987]; [LeBertre 1987; LeBertre 1988b; LeBertre 1988a]; [Griffin 1990]; [Orofino *et al.* 1990]) e.g. implies the presence of amorphous grains rather than graphite in the circumstellar shells around C-stars. This is consistent with physical considerations, predicting the formation of inhomogeneous grains with crystalline cores surrounded by amorphous mantles ([Gail and Sedlmayr 1984]), as only the mantles interact with the radiation field.

The observations further indicate, that most dust enshrouded AGB stars are LPVs or Miras [Jura 1986b], [Habing 1990]. Therefore, a two–step mechanism has been proposed as being responsible for the mass loss of LPVs ([Jones *et al.* 1981]): i) levitation of the atmosphere by dissipation of shock waves, and ii) subsequent acceleration of the material by radiation pressure on dust grains.

Besides the fundamental work concerning AGB stars, an impressive list of mass loss rates of objects throughout the HR-diagram is given in [deJager *et al.* 1988] where also empirical formulas are derived for expressing the observed mass loss rates $\dot{M}$ as function of the corresponding fundamental stellar parameters. While the paper of deJager essentially concentrates on M–stars, [Olofsson *et al.* 1993a], [Olofsson *et al.* 1993b] have collected an extensive survey regarding the structure, the mass loss rates and the molecular abundances of cool C–star envelopes, thus establishing a save basis and reliable boundary conditions for the future theoretical investigations of these objects.

We further mention a recent paper of [Habing *et al.* 1994] which is concerned with the outflow velocities of cool giants and supergiants, where semi-empirical formulas for the observed mass loss rate and for the terminal wind velocity are given for various situations by discussing basically a three component model (gas, dust and photons).

Regarding the spatial structure of circumstellar dust shells, detailed information is obtained by interferometric measurements or lunar occultation data (e.g. [Sutton *et al.* 1977], [Sutton *et al.* 1978], [Sutton *et al.* 1979], [McCarthy *et al.* 1980], [Dyck *et al.* 1984], [Dyck *et al.* 1987], [Dyck *et al.* 1991], [Dyck *et al.* 1992], [Ridgway *et al.* 1986], [Ridgway and Keady 1988], [Danchi *et al.* 1990; Danchi *et al.* 1994]) from which the position of the onset of dust formation and the dust temperature in the formation zone can be deduced (e.g. [Danchi *et al.* 1990]).

In summarizing the basic results, all these investigations indicate that dust induced mass loss is a very natural phenomenon which is expected for objects having high luminosity ($L_* \gtrsim 5 \cdot 10^3 L_\odot$), low effective temperature ($T_* \lesssim 3000$ K), large mass loss rates ($\dot{M} \gtrsim 10^{-6} M_\odot \mathrm{yr}^{-1}$) and small outflow velocities ($v_\infty \leq 40\,\mathrm{kms}^{-1}$), a fact which is in good agreement with the theoretical arguments given in Sect. 3.3 and the results of the model calculations presented in Sect. 6.

3 Theoretical description of a dust driven wind

3.1 Fundamental ingredients

The selfconsistent formulation of a dust driven wind requires the simultaneous treatment of four closely coupled nonlinear complexes of very different nature. Fig. 1 depicts these problems and their mutual basic coupling which is essential for the realistic modelling of the shell structure and the quantitative understanding of the wind generation.

The most important coupling in this system is provided by the *dust–photon interaction* which determines both the hydrodynamic and the thermodynamic structure of the shell. However, as the dust condensation process very sensitively depends on the local temperature and molecular density, a realistic calculation of the dust absorption requires the detailed treatment of the dust formation process which again is only possible on the basis of a reliable shell structure and a realistic shell chemistry.

3.2 Basic equations

The standard scenario for describing a stellar wind is to consider a stationary, spherically symmetric outflow. For the usual situation of a long lasting steady mass loss ($10^4 \ldots 10^6$ yr) both assumptions seem to be justified because i) the intrinsic time scales governing the local physics are short compared to the time scale of the global wind variation, and ii) the typical amplitudes of fluctuations are small compared to the corresponding mean values. However, in special cases, where pulsations and shock waves play an important role, the assumption of stationarity might not be justified. Also the assumption of spherical symmetry is questionable if in the extended shell significant local inhomogeneities like dust clouds appear (e.g. RCrB stars) or if the dust formation is confined to some particular non-spherical region as e.g. to the equatorial disk of B[e]-stars.

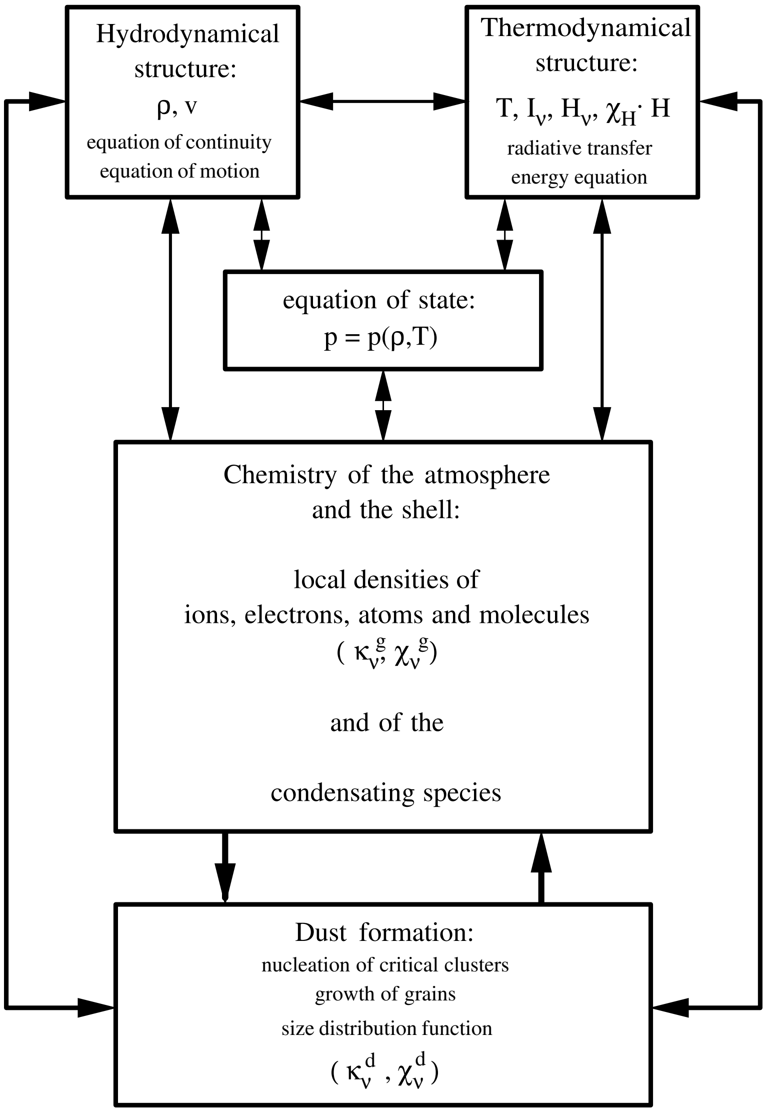

Fig. 1. Selfconsistent description of a dustforming circumstellar shell exhibiting the basic couplings of the various complexes involved (after Sedlmayr and Winters 1991).

However, throughout this paper we are mainly referring to the *standard case* defined by adopting a *one fluid system, stationarity* and *spherical symmetry.*

3.2.1 The hydrodynamic equations

The basic equations describing the hydrodynamical and thermodynamical structure of the shell are provided by the local conservation laws:

a) *Mass conservation*

Mass conservation is expressed by the equation of continuity

$$\frac{1}{r^2}\frac{\partial}{\partial r}(r^2 \rho v) = 0, \tag{3.1}$$

where r is the radial coordinate, $\rho(r)$ the local mass density and $v(r)$ the local hydrodynamical velocity.

Integration of Eq. (3.1) over a sphere with radius r immediately yields the integral form of mass conservation

$$4\pi r^2 \rho v = \dot{M} \tag{3.2}$$

with the constant of integration $\dot{M}$ which measures the total transport of mass through the surface of the considered sphere and, therefore, is the *mass loss rate* of the star.

In selfconsistent wind models, $\dot{M}$ results as a global quantity which is essentially determined by the fundamental parameters of the star: mass M_*, effective temperature T_*, luminosity L_* and chemical abundances $\{\epsilon_\ell\}$.

Until now, selfconsistent solutions for the mass loss rate exist only for purely radiation driven winds where the basic mechanisms for wind generation are explored and realistic quantitative descriptions are available.

For the situation of pressure driven winds, however, no selfconsistent solutions exist and one still has to refer to the empirical *Reimers formula* (e.g. [Reimers 1975])

$$\dot{M} = 4 \cdot 10^{-13} \frac{L_*}{L_\odot} \cdot \frac{M_\odot}{M_*} \cdot \frac{R_*}{R_\odot} \tag{3.3}$$

which expresses the mass loss rate by the fundamental stellar parameters luminosity, mass, and radius measured in solar units $L_\odot$, $M_\odot$ and $R_\odot$.

Relation (3.3) has been derived by studying a large sample of cool stars consisting mostly of K and early M giants showing moderate mass loss rates. Despite large individual deviations, the Reimers formula can be considered as a reliable quantitative description of the mass loss rate in this regime. However, in many important situations – like pulsational variables, giants and supergiants along the AGB, and cool heavily dust obscured objects – relation (3.3) may be severely in error. For an application of the Reimers formula also in such situations, usually relation (3.3) is multiplied by a suitable scaling factor in order to yield the observed mass loss rate.

b) *Momentum conservation*

Momentum conservation is provided by the equation of motion

$$v\frac{\partial v}{\partial r} = -\frac{1}{\rho}\frac{\partial p}{\partial r} + a \tag{3.4}$$

with $p(r)$ being the thermal pressure and $a(r)$ the net acceleration of the matter due to external forces.

Under the conditions of a wind, the thermal pressure is given by the ideal gas law

$$p = \frac{\rho}{\bar{\mu} m_p} kT \tag{3.5}$$

where $\bar{\mu}(r)$ is the local mean molecular weight, m_p the proton mass, $T(r)$ the local kinetic temperature and k the Boltzmann constant.

The acceleration $a(r)$ due to external forces consists of two terms

$$a = -g + a_{rad} \tag{3.6}$$

where $-g$ is the local inwards directed gravitational acceleration and $a_{rad}(r)$ is the local outwards directed acceleration caused by the radiation field of the star

$$a_{rad} = \frac{4\pi}{c}\frac{\chi_H}{\rho} H \tag{3.7a}$$

where H is the frequency integrated Eddington flux H_ν (see Eq. 3.44), and χ_H is the corresponding flux average of the monochromatic extinction coefficient χ_ν (see Eq. 3.54).

The gravitational acceleration is conceived to originate from two contributions

$$g(r) = G\frac{M_* + M_s(r)}{r^2} \quad , \tag{3.8}$$

where M_* is the mass of the central star having radius R_* and

$$M_s(r) = \int_{R_*}^{r} dr' r'^2 \rho(r') \tag{3.9}$$

is the mass contained in the circumstellar shell of radius r. By this definition, two important conceptual problems arise:

i) Due to the mass loss, M_* is a slowly decreasing function of time. This time variation only can be ignored if the corresponding mass loss time scale $M_*/\dot{M}$ is small compared to the timescale controlling the global shell expansion d/v, where d is the shell dimension and v the expansion velocity. Adopting typical values $d \simeq 10^{17}$ cm and $v \simeq 20\,\mathrm{kms}^{-1}$ shows that this condition requires $M_*/\dot{M} < 10^3$ yr. This inequality is only violated for objects having very small mass and extremely large mass loss rates.

ii) As the expansion velocity of the wind rather soon approaches a nearly constant value (the terminal velocity), in the free expansion region the density ρ decreases like r^{-2}. For this reason, $M_s(r)$ increases proportional to the shell extension. Since M_s has to be bounded by the initial stellar mass, the dimension of the shell should be confined within some suitably defined maximum radius (e.g. by the position of the shock in the transition region between wind and interstellar medium).

These problems clearly indicate the limits of the applicability of a stationary approach.

An additional question concerns the consistent definition of the stellar radius R_* for objects having extended atmospheres. This important problem is discussed in [Baschek *et al.* 1991] and in the context of carbon stars by [Jørgensen *et al.* 1992]. Our definition adopted in this paper refers to the approach of [Lucy 1971], [Lucy 1976], where R_* is determined as an eigenvalue of the system (A.11) and (A.13), fulfilling condition (A.23). This definition, however, is only compatible with the above definition of M_* if $R_* < r_d$ holds, with r_d being the inner radius of the dust formation region, a condition which is violated only for the most obscured objects showing very heavy mass loss. In this case, the above distinction between the central stellar object and the surrounding dust shell is meaningless and a more adequate description of the object based on its global properties is necessary. Such an approach, which has to incorporate the full hydrodynamics, chemistry and radiative transfer is not at hand up to now.

In practical calculations, Eq. (3.6) usually is written as

$$a = -g\,(1-\alpha) \tag{3.10}$$

with

$$\alpha(r) = \frac{a_{rad}}{g} = \frac{4\pi}{cG\rho M_*}\,\chi_H r^2 H \tag{3.7b}$$

being the radiative acceleration measured in units of the corresponding local gravity.

As the mass extinction coefficient of solid particles is several orders of magnitude larger than that of gaseous matter, χ_H is essentially given by the dust component (cf. Eq. (3.71)), whenever significant fractions of dust are present.

Equations (3.7) only are correct, however, if the photons' momentum absorbed by the grains is immediately transferred to the ambient gas via a close collisional coupling between the gas and the dust components. This means in particular that no significant drift of dust particles relative to the mean mass system should occur. If grain–gas momentum coupling is not complete, a two component description of the wind hydrodynamics has to be applied. This idea has been put forward by ([Berruyer and Frisch 1983], [Berruyer 1991] and [MacGregor and Stencel 1992]) who discuss the effects of grain drift and incomplete gas–dust coupling in circumstellar dust shells. These results, which affect in particular the small grain limit, indicate that significant momentum decoupling only is to be expected for mass loss rates $\dot{M} \lesssim 10^{-8} M_{\odot}\mathrm{yr}^{-1}$. Such low mass loss rates are well below the limit line for purely dust driven winds to occur (see Sect. 3.3.2). For this reason, we feel justified to adopt Eqs. (3.7) as a reliable approximation for the radiative wind acceleration (see also [Dominik *et al.* 1990]).

By means of the isothermal sound velocity

$$c_T^2 = \frac{p}{\rho} \tag{3.11}$$

and the equation of continuity (3.1), Eq. (3.4) can be immediately transformed into the usual form of a *wind equation*

$$(v^2 - c_T^2)\,\frac{1}{v}\,\frac{\partial v}{\partial r} = \frac{2}{r}\,c_T^2 - \frac{\partial c_T^2}{\partial r} - g(1-\alpha) \tag{3.12}$$

with the critical point r_c defined by the conditions

$$v(r_c) = c_T(r_c) \tag{3.13}$$

and

$$\frac{2}{r_c}\,c_T^2(r_c) - \frac{\partial c_T^2}{\partial r}|_{r_c} - g(r_c)(1-\alpha(r_c)) = 0 \quad . \tag{3.14}$$

If we neglect the temperature variation in Eq. (3.14), the position r_c of the critical point is determined by the implicit equation

$$\alpha(r_c) = 1 - 4\,\frac{r_c}{R_*}\left(\frac{c_T(r_c)}{v_e}\right)^2 \tag{3.15}$$

with

$$v_e = (2R_* g(R_*))^{1/2} \tag{3.16}$$

being the *escape velocity* at the stellar surface. For a small star, v_e always has to be large compared to c_T in order to prevent thermal evaporation (cf. [Gail 1990]).

In case of dust driven winds, $\alpha(r)$ increases steeply from values $\alpha \ll 1$ at the onset of dust formation to values $\alpha > 1$ in the inner wind zone. This transition zone of α defines a rather narrow region where the critical point has to be situated. Selfconsistent model calculations indicate that for dust driven mass loss the second term in Eq. (3.15) always is small compared to unity and, thus,

$$\alpha(r_c) \simeq 1 \tag{3.17}$$

is a necessary condition for a dust driven wind to exist. This condition confirms that dust condensation is responsible for generating the mass loss and for driving the wind.

In case of continuous mechanical momentum input, the equation of motion is slightly modified by introduction of an additional wave force density

$$\boldsymbol{f}_w = div\ \boldsymbol{p}_w \quad , \tag{3.18}$$

with $\boldsymbol{p}_w$ being a properly defined wave pressure tensor (cf. [Holzer and MacGregor 1985]). For spherical symmetry, $\boldsymbol{f}_w$ reduces to

$$f_w = \frac{1}{r^2}\frac{\partial}{\partial r}(r^2 p_{w,r}) \tag{3.18a}$$

with $p_{w,r}$ being the radial part of $\boldsymbol{p}_w$.

According to [Pijpers and Habing 1989], $p_{w,r}$ is adopted to be some fraction of the thermal pressure

$$p_{w,r} = \delta \cdot p \tag{3.19}$$

where the dimensionless parameter $\delta > 0$ measures the relative momentum contribution due to the wave dissipation. δ is assumed to be constant throughout the wind zone.

Inserting Eqs. (3.18a) and (3.19) into Eq. (3.4) results in the wind equation

$$\left[v^2 - (1+\delta)c_T^2\right]\frac{1}{v}\frac{\partial v}{\partial r} = \frac{2c_T^2}{r} - (1+\delta)\frac{\partial c_T^2}{\partial r} - g(1-\alpha) \tag{3.12a}$$

with the consequence that for $\delta > 0$ the critical point r_c of the velocity field

$$v(r_c) = v_c = (1+\delta)^{1/2} c_T(r_c) \tag{3.20}$$

is shifted outwards, a fact which favours dust formation. From Eq. (3.12a) one confers that under the above assumption of neglecting the temperature dependence of c_T, conclusion (3.17) remains valid without modification.

c) *Energy conservation*

The energy balance in our system is given by the equation for the thermal energy

$$v\left(\rho c_p \frac{\partial T}{\partial r} - \frac{\partial p}{\partial r}\right) = Q_e \tag{3.21}$$

with c_p being the specific heat for constant pressure, and $Q_e(r)$ the local net energy input rate per unit volume due to external energy sources. The l.h.s. of Eq. (3.21) accounts for both the variation of the local specific enthalpy and for the work of the pressure forces. As shock waves are not considered in our simple flow system, heat conduction is neglected in Eq. (3.21). For dust driven winds, the expansion velocity and also the temperature and pressure gradients are small compared to the source terms provided by the stellar radiation field. Then the energy equation (3.21) reduces to the situation of *radiative equilibrium* which is defined by the local balancing of radiative heating and cooling

$$Q_e = \Gamma_e - \Lambda_e = 0 \tag{3.22}$$

where $\Gamma_e(r)$ and $\Lambda_e(r)$ describe the local energy gain and loss rates, respectively.

Throughout this paper we adopt *conservative scattering* of radiation. Therefore, in radiative equilibrium, energy conservation is simply given by the overall balance of absorption and emission processes per volume and time

$$\int_0^\infty d\nu \kappa_\nu J_\nu = \int_0^\infty d\nu \epsilon_\nu \quad , \tag{3.23}$$

where ϵ_ν is the spectral emission coefficient of the matter and $J_\nu(r)$ the local mean intensity of the radiation field defined by Eq. (3.43).

Under the condition of LTE, *Kirchhoff's* law

$$\epsilon_\nu = \kappa_\nu B_\nu(T) \tag{3.24}$$

holds, where $B_\nu(T)$ is the Planck function with the local equilibrium temperature $T(r)$. In this case, radiative equilibrium is expressed by the equation

$$\int_0^\infty d\nu \kappa_\nu J_\nu = \int_0^\infty d\nu \kappa_\nu B_\nu(T) \quad . \tag{3.25}$$

By defining appropriate mean absorption coefficients

$$\kappa_J = \frac{1}{J}\int_0^\infty d\nu \kappa_\nu J_\nu \quad \text{and} \quad \kappa_B = \frac{1}{B}\int_0^\infty d\nu \kappa_\nu B_\nu \tag{3.26}$$

with $J(r)$ and $B(r)$ denoting the frequency integrated quantities J_ν and B_ν, respectively, Eq. (3.25) can be rewritten as

$$\kappa_J J = \kappa_B B(T) \tag{3.27}$$

which by means of the *Stefan-Boltzmann* law

$$B(T) = \frac{\sigma}{\pi} T^4 \tag{3.28}$$

where σ is the Stefan-Boltzmann constant, yields the (equilibrium) temperature structure

$$T^4 = \frac{\pi}{\sigma}\frac{\kappa_J}{\kappa_B} J \quad . \tag{3.29}$$

In a first approximation, a dusty shell physically has to be considered as a two component system consisting of gas and dust which generally is *not* in a state of thermal equilibrium. In particular, the internal temperature of the dust grains $T_d(r)$ may be significantly different from the temperature of the gas particles $T_g(r)$ due to a pronounced *greenhouse effect.* In this case, the condition of radiative equilibrium is given by

$$\int_0^\infty d\nu (\kappa_\nu^g + \kappa_\nu^d) J_\nu = \int_0^\infty d\nu (\epsilon_\nu^g + \epsilon_\nu^d) \tag{3.30}$$

with g and d denoting the gas and the dust component, respectively. Introducing the *gas source function*

$$S_\nu^g = \frac{\epsilon_\nu^g}{\kappa_\nu^g} \tag{3.31}$$

and assuming thermal emission of the dust particles with internal temperature T_d, Eq. (3.30) can be rewritten as

$$\int_0^\infty d\nu (\kappa_\nu^g + \kappa_\nu^d) J_\nu = \int_0^\infty d\nu (\kappa_\nu^g S_\nu^g + \kappa_\nu^d B_\nu(T_d)) \quad . \tag{3.32}$$

If the dust component energetically decouples from the gas system, the dust temperature $T_d(r)$ is determined by the energy balance for the dust component alone

$$\int_0^\infty d\nu \kappa_\nu^d J_\nu = \int_0^\infty d\nu \kappa_\nu^d B_\nu(T_d) \quad . \tag{3.33}$$

Assuming equilibrium between the various gas components, S_ν^g is a function of the local gas temperature $T_g(r)$ only. Then, by means of the implicit equations (3.32) and (3.33), the gas temperature T_g and the dust temperature T_d can be calculated. Depending on the grain component considered in model calculations of dust shells, $T_d(r)$ results to be either larger (e.g. for amorphous carbon) or smaller (e.g. for SiC- and PAH-particles) than $T_g(r)$, thus showing a positive or an *inverse greenhouse effect*, respectively.

3.2.2 Radiative Transfer

a) *The transfer equation*

The propagation of radiation along a ray $\boldsymbol{\xi} = \xi\hat{\boldsymbol{\xi}}$ is described by the transfer equation for the local monochromatic specific intensity $I_\nu(\boldsymbol{\xi}) = I_\nu(\xi, \hat{\boldsymbol{\xi}})$, where ξ defines the position on an arbitrarily chosen light ray and $\hat{\boldsymbol{\xi}}$ its direction:

$$\frac{dI_\nu}{d\xi} = -(\kappa_\nu + s_\nu)\, I_\nu + \epsilon_\nu + \frac{1}{4\pi}\int d\Omega' s_\nu I_\nu(\xi, \hat{\boldsymbol{\xi}}') \tag{3.34}$$

with $\kappa_\nu(\boldsymbol{\xi}), s_\nu(\boldsymbol{\xi}), \epsilon_\nu(\boldsymbol{\xi})$ being the coefficients for absorption, elastic scattering and emission of the matter. $d\Omega'$ in the scattering integral denotes the element of solid angle.

By assuming isotropic absorption, scattering and emission, Eq. (3.34) reduces to

$$\frac{dI_\nu}{d\xi} = -(\kappa_\nu + s_\nu)\, I_\nu + \epsilon_\nu + s_\nu \frac{1}{4\pi}\int d\Omega' I_\nu(\xi, \hat{\boldsymbol{\xi}}') \tag{3.35}$$

which by introduction of the local mean intensity

$$J_\nu(\xi) = \frac{1}{4\pi}\int d\Omega' I_\nu(\xi, \hat{\boldsymbol{\xi}}) \tag{3.36}$$

results to

$$\frac{dI_\nu}{d\xi} = -(\kappa_\nu + s_\nu)\, I_\nu + \epsilon_\nu + s_\nu J_\nu \quad , \tag{3.37}$$

where all quantities are functions of the position ξ on the ray only. Due to the scattering integral, Eq. (3.37) is an ordinary integro-differential equation of first order.

For spherically symmetric systems, $\boldsymbol{\xi}$ is expressed by spherical coordinates (r, ϑ, φ), with r being the radial distance, ϑ the angle between the radius vector and the direction of light propagation, and φ the azimut which due to spherical symmetry is redundant in this case.

By this coordinate transformation, the specific intensity $I_\nu(\xi, \hat{\boldsymbol{\xi}})$ changes to $I_\nu(r, \vartheta)$ obeying the transfer equation

$$\mu \frac{\partial I_\nu}{\partial r} + \frac{1-\mu^2}{r} \frac{\partial I_\nu}{\partial \mu} = -(\kappa_\nu + s_\nu) I_\nu + \epsilon_\nu + s_\nu J_\nu \tag{3.38}$$

where the transport coefficients κ_ν, s_ν and ϵ_ν are functions of r only. $\mu = \cos\vartheta$ denotes the angle variable.

Equation (3.38) is the standard form for the equation of radiative transfer applied in calculations of spherical dust shells.

A particular simple transfer equation results if scattering can be neglected

$$\mu \frac{\partial I_\nu}{\partial r} + \frac{1-\mu^2}{r} \frac{\partial I_\nu}{\partial \mu} = -\kappa_\nu I_\nu + \epsilon_\nu \quad . \tag{3.39}$$

As in cool envelopes scattering is dominantly caused by dust particles, Eq. (3.39) is an appropriate approximation for the innermost region of the shell where dust is absent.

b) *The moment equations*

Instead of a direct numerical solution of Eq. (3.38), in many situations it is advantageous to solve the corresponding system of *moment equations* which follows from Eq. (3.38) by multiplication with μ^n and subsequent angle integration over the full range for $n = 0, 1, 2, \ldots$, respectively.

By definition of *angular moments* of the local specific intensity (*Eddington moments*)

$$M_\nu^n(r) = \frac{1}{2} \int_{-1}^{+1} d\mu \mu^n I_\nu(r, \mu) \quad , \tag{3.40}$$

the transfer equation (3.38) is represented by an infinite system of moment equations

$$\frac{\partial M_\nu^{n+1}}{\partial r} + \frac{n+2}{r} M_\nu^{n+1} - \frac{n}{r} M_\nu^{n-1} = -(\kappa_\nu + s_\nu)\, M_\nu^n + \begin{cases} \frac{1}{n+1}(\epsilon_\nu + s_\nu M_\nu^0) & \text{for } n \text{ even} \\ 0 & \text{for } n \text{ odd} \end{cases} \quad n = 0, 1, 2, \ldots \tag{3.41}$$

As the n-th equation always contains the $(n+1)$-th moment, the system (3.41) has to be completed by an appropriate *closure condition* at some sufficiently large $n = n_{max}$

$$M_\nu^{n_{max}+1} = \phi(M_\nu^0, \ldots, M_\nu^{n_{max}}) \tag{3.42}$$

by which the moment $M_\nu^{n_{max}+1}$ is expressed by lower moments.

For practical applications $n_{max} = 1$ is the usual approximation. In this case only the three moments

- *mean intensity*

$$J_\nu = M_\nu^0 = \frac{1}{2} \int_{-1}^{+1} d\mu I_\nu(r, \mu) \tag{3.43}$$

- *Eddington flux*

$$H_\nu = M_\nu^1 = \frac{1}{2} \int_{-1}^{+1} d\mu \mu I_\nu(r, \mu) \tag{3.44}$$

- *Eddington pressure*

$$P_\nu = M_\nu^2 = \frac{1}{2} \int_{-1}^{+1} d\mu \mu^2 I_\nu(r, \mu) \tag{3.45}$$

are involved.

Eddington flux and Eddington pressure correspond directly to the spectral flux of *radiative energy*

$$F_\nu = 4\pi H_\nu \tag{3.46}$$

and to the *spectral radiative pressure tensor* $p_{ik}(\nu)$ which in case of isotropic radiation simply is given by

$$p_{ik}(\nu) = \frac{4\pi}{c}\, P_\nu \delta_{ik} \tag{3.47}$$

where δ_{ik} is the isotropic unit tensor.

For $n_{max} = 1$ and with the definitions (3.43), (3.44) and (3.45), the system of moment equations (3.41) reduces to a set of two coupled ordinary differential equations

$$\frac{\partial H_\nu}{\partial r} + \frac{2}{r} H_\nu = -\kappa_\nu J_\nu + \epsilon_\nu \tag{3.48}$$

$$\frac{\partial P_\nu}{\partial r} + \frac{1}{r}(3P_\nu - J_\nu) = -(\kappa_\nu + s_\nu) H_\nu \tag{3.49}$$

which is closed by the introduction of a so-called *variable Eddington factor* $f_\nu(r)$ expressing the Eddington pressure at each point by the corresponding mean intensity

$$P_\nu(r) = f_\nu(r) J_\nu(r) \tag{3.50}$$

which in Eq. (3.49) allows a formal elimination of P_ν in terms of J_ν.

Limiting values for f_ν are

$$f_\nu = \begin{cases} \frac{1}{3} & \text{for isotropic radiation} \\ 1 & \text{for radially directed radiation.} \end{cases} \tag{3.51}$$

For the realistic situation in an extended shell, f_ν has to be determined by an iteration procedure.

Frequency integration of Eqs. (3.48) and (3.49) yields

$$\frac{\partial H}{\partial r} + \frac{2}{r} H = -\int_0^\infty d\nu \kappa_\nu J_\nu + \int_0^\infty d\nu\, \epsilon_\nu \tag{3.52}$$

$$\frac{\partial P}{\partial r} + \frac{1}{r}(3P - J) = -\int_0^\infty d\nu (\kappa_\nu + s_\nu) H_\nu = -\chi_H H \quad , \tag{3.53}$$

with χ_H being the flux average of the extinction coefficient $\chi_\nu = \kappa_\nu + s_\nu$:

$$\chi_H = \frac{1}{H} \int_0^\infty d\nu \chi_\nu H_\nu \ . \tag{3.54}$$

In case of radiative equilibrium, the r.h.s. of Eq. (3.52) is zero according to Eqs. (3.23) and (3.52) reduces to

$$\frac{1}{r^2} \frac{\partial}{\partial r}(r^2 H) = 0 \tag{3.55}$$

which describes the conservation of the total radiative flux H. Solution of Eq. (3.55) yields

$$H = H_* \left(\frac{R_*}{r}\right)^2 \tag{3.56}$$

with the constant of integration

$$H_* = \frac{L_*}{16\pi^2 R_*^2} = \frac{\sigma}{4\pi} T_*^4 \tag{3.57}$$

being the corresponding flux value at radius $r = R_*$, expressed by the stellar luminosity L_* and the effective temperature T_*, respectively.

A very simple and powerful method for an approximate treatment of radiative transfer in an extended shell has been introduced by [Lucy 1971], [Lucy 1976] which yields reliable results for so called optically thin shells, for which the "diluted" optical depth $\tau_L(R_*)$ of the entire dust shell (cf. (A.23)) allows an eigenvalue R_* smaller than the radius r_d of the inner edge of the dust forming region. As the Lucy-approximation is still widely used for treating radiative transfer in an extended shell, it is outlined in the Appendix.

3.2.3 Transport coefficients

a) *Gas absorption*

The radiative transfer in cool stellar atmospheres is dominated by photon interaction with the molecules present. Compared to hot systems, this introduces big problems not only due to the huge number of transitions to be taken into account but also due to the difficulty of determining reliable molecular abundances, which in many cases depart considerably from chemical equilibrium (see Sect. 4.1). For this reason, up to now no consistent values for the total molecular absorption coefficients κ_ν^g exist for a cool stellar envelope (see e.g. the excellent reviews of [Tsuji 1986] and [Gustafsson 1989].

Nevertheless, in the last years, impressive progress has been achieved, both in calculating molecular opacities by means of quantum mechanical treatments and by laboratory measurements of the important molecules (see the corresponding proceedings on astrophysical opacities, e.g. [Lynas-Gray *et al.* 1992] and [Jørgensen 1994]) and by developing efficient statistical techniques which allow to obtain reliable frequency dependent opacity coefficients for relevant molecules like OH, CN, TiO, H_2O, etc. These treatments either use suitably defined *opacity distribution functions* (ODF) or reliable *opacity sampling methods* (OF) in order to account qualitatively for the huge number of transitions which contribute to the absorption coefficient of a molecule (e.g. [Querci *et al.* 1974], [Johnson *et al.* 1980], [Carbon 1979], [Carbon 1984], [Ekberg *et al.* 1986], [Alexander *et al.* 1989] and [Allard *et al.* 1992]). In this context, we refer to the review of [Johnson 1986] and in particular to the work on molecular opacities of our Scandinavian colleagues at Copenhagen and Uppsala (cf. [Jørgensen 1992a; Jørgensen 1992b; Jørgensen 1994] and [Plez *et al.* 1992] and references therein), but also to the large progress achieved by the big efforts of [Kurucz 1994] in the last decade.

b) *Dust absorption and scattering*

In those regions of a circumstellar shell where dust is present, the extinction of the dust component usually is orders of magnitudes larger than that of the gas component. This is due to both the large geometrical cross sections of the grains and the high extinction efficiencies of astrophysical solids like silicate or carbon compounds.

The absorption and extinction cross sections of three–dimensional solid particles can be calculated by means of the *Mie-theory* for given size and shape of the grains and given complex index of refraction of the grain material $m(\lambda) = n(\lambda) - ik(\lambda)$, with $n(\lambda)$ being the refraction index and $k(\lambda)$ the corresponding dissipative contribution for photons with wavelength λ.

Assuming spherical particles with radius a and isotropic scattering, the monochromatic extinction cross section $\sigma^d_{ext}(\lambda, a)$ and the scattering cross section $\sigma^d_{sca}(\lambda, a)$ can be calculated analytically by series expansions (e.g. [Kerker 1969], [Bohren and Huffman 1983]).

On the basis of these cross sections, the extinction, scattering and absorption coefficients for the dust component follow immediately by integration over the local radius size distribution function $f(a)$ of the grains (cf. [Dominik *et al.* 1989]), with $f(a)da$ being the number density of the grains having a radius between $(a, a + da)$:

grain extinction coefficient:

$$\chi^d_\lambda = \int da f(a) \sigma^d_{ext}(\lambda, a) \tag{3.58}$$

grain scattering coefficient:

$$s^d_\lambda = \int da f(a) \sigma^d_{sca}(\lambda, a) \tag{3.59}$$

grain absorption coefficient:

$$\kappa^d_\lambda = \int da f(a) \sigma^d_{abs}(\lambda, a) = \chi^d_\lambda - s^d_\lambda \quad . \tag{3.60}$$

These formulas are given for one grain component. In case that additional grain components are present, their individual contributions simply have to be added.

Particular simple expressions result for the *small particle limit* $a \ll \lambda/2\pi$ and the *large particle limit* $a \gg \lambda/2\pi$, respectively, where the cross sections for absorption and scattering are given by simple analytic relations. In the small particle limit

$$\sigma^d_{abs} = A(\lambda) a^3 \tag{3.61}$$

and

$$\sigma^d_{sca} = B(\lambda) a^6 \tag{3.62}$$

with the wavelength dependent material functions

$$A(\lambda) = -\frac{8\pi^2}{\lambda} \,\Im \left(\frac{m^2 - 1}{m^2 + 2} \right) \tag{3.63a}$$

and

$$B(\lambda) = \frac{128\pi^5}{3\lambda^4} \,\Re \left(\frac{m^2 - 1}{m^2 + 2} \right) \quad , \tag{3.63b}$$

where $\Im$ and $\Re$ denote the imaginary and the real part of the bracket expression, respectively. In this case, the corresponding transport coefficients are immediately expressed by suitably defined *moments* (cf. Eq. (5.19))

$$K_j = \int da a^j \, f(a) \qquad j = 0, 1, 2, \ldots \tag{3.64}$$

of the radius distribution function $f(a)$ (see Sect. 5.3):

$$\kappa^d_\lambda = A(\lambda) \int da a^3 \, f(a) = A(\lambda) K_3 \tag{3.65}$$

$$s^d_\lambda = B(\lambda) \int da a^6 \, f(a) = B(\lambda) K_6 \tag{3.66}$$

and

$$\chi^d_\lambda = \kappa^d_\lambda + s^d_\lambda \quad . \tag{3.60}$$

In the large particle limit, both the absorption and the scattering cross section approach the *geometrical* cross section of the particle

$$\sigma^d_{geo}(a, \lambda) = \sigma^d_{abs}(a, \lambda) = \sigma^d_{sca}(a, \lambda) = \pi a^2 \tag{3.67}$$

which is independent of the wavelength λ. In this case, the corresponding transport coefficients are simply given by

$$\kappa^d_\lambda = s^d_\lambda = \pi \int da a^2 \, f(a) = \pi K_2 \tag{3.68}$$

and

$$\chi^d_\lambda = 2 \, \kappa^d_\lambda \quad . \tag{3.69}$$

Selfconsistent models of dust shells indicate that reliable results for the dust absorption coefficient are obtained

- by using the large particle limit in the innermost region of the dust shell, and
- by using the small particle limit in the outermost region of the dust shell,

because in the innermost region of the dust shell both gas density and collision frequency are large, thus providing excellent growth conditions, whereas in the outermost regions, due to the progressing dilution and cooling of the gas, the growth conditions become unfavourable (cf. Fig. 8).

For the extended wind zone in between, always the full expression (3.60) has to be applied (cf. [Sedlmayr and Winters 1991]). For the calculation of the dust scattering coefficient, these limit approximations are severely in error in the entire wind region. Therefore, if scattering is included, one always has to rely on the exact equation (3.59). In any case, the calculation of the transport coefficients due to dust involves the treatment of the extremely nonlinear problem sketched in Fig. 1.

3.3 Global condition for the existence of dust driven winds

3.3.1 Stabilizing control circuits

By this circular coupling, both for momentum and energy, stabilizing control circuits are induced by dust formation which guarantee that in case of stationary dust driven winds, the shell remains stable, in contrast to non-monotonic situations like Miras and LPVs or RCrB stars where instabilities develop. Fig. 2 gives schematic flow charts illustrating these negative, i.e. stabilizing feed backs of energy and momentum flow in case of dust driven winds.

3.3.2 The minimum mass loss rate

Insertion of Eqs. (3.55) and (3.56) into Eq. (3.7b) allows to express the relative radiative acceleration α by the fundamental stellar parameters mass and luminosity

$$\alpha = \frac{\chi_H}{4\pi c G \rho M_*} L_* \quad . \tag{3.70}$$

Within dust shells, the gas extinction is negligible compared to the corresponding dust contribution. Thus, χ_H in Eq. (3.70) is essentially given by χ_H^d, the flux average of the local dust extinction coefficient

$$\chi_H^d = \frac{1}{H}\int_0^\infty d\nu H_\nu \int da\, f(a)\sigma_{ext}^d(\nu, a) \quad , \tag{3.71}$$

which shows a complicated implicit dependence on both the size distribution of the grains and the frequency spectrum of the radiation field.

In Sect. 3.2.1 b), it has been demonstrated that $\alpha(r_c) \simeq 1$ (Eq. (3.17)) is a necessary condition for a dust driven wind to exist. Therefore, χ_H^d has to be evaluated in the vicinity of the critical point r_c, i.e. in the innermost region of

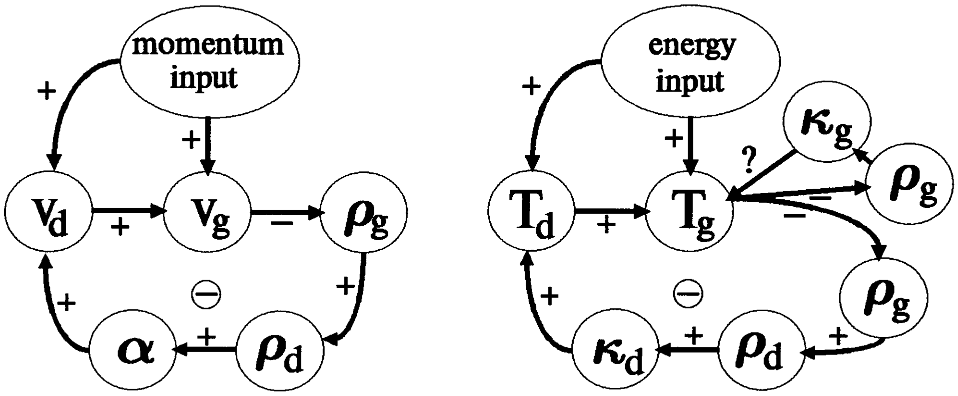

Fig. 2. Stabilizing control circuits for momentum and energy induced by dust condensation in a stellar wind. Quantities with index g(d) refer to the gas (dust)-component, respectively. The negative sign of the product of the influences (symbolised by the arrows) in a closed loop guaranties dynamical and thermal stability of the system. The side chain of the energy circuit indicated by ? depends strongly on the actual form of κ_g. Thus, its influence upon T_g can be positive or negative. However, this fact does not alter the above general conclusion (adopted from [Sedlmayr 1994]).

the dust shell. There the grains are large and the large particle limit is a good approximation for calculating χ_H^d. Inserting Eqs. (3.71) and (3.68) into Eq. (3.70) yields

$$\alpha = \frac{K_2}{2cG\rho M_*} L_* \quad . \tag{3.72}$$

In the vicinity of r_c, the particle size distribution function $f(a)$ can be approximated by a power law

$$f(a) \propto a^{-\beta} \tag{3.73}$$

with exponent β slightly larger than +4 (see [Dominik *et al.* 1989], cf. also Sect. 6.2).

In this case, K_2 is approximately proportional to the *degree of condensation*

$$\gamma = \frac{K_3}{K_{3,max}} \quad , \tag{3.74}$$

where K_3 describes the actual amount of condensed material (3-dimensional grains) and $K_{3,max}$ its corresponding value if *all* condensable material would have condensed into grains, which implies the simple relation

$$K_2 = \gamma K_{2,max} \quad . \tag{3.75}$$

Elimination of K_2 in Eq. (3.72) by means of Eq. (3.75) yields

$$\alpha = \gamma \, \frac{K_{2,max}}{2cG\rho M_*} \, L_* \quad , \tag{3.76}$$

which by introduction of the Eddington-luminosity

$$L_{edd} = \frac{4\pi c G\rho M_*}{\chi_{H,max}} = \frac{2cG\rho M_*}{K_{2,max}} \tag{3.77}$$

results to

$$\alpha = \gamma \, \frac{L_*}{L_{edd}} \quad . \tag{3.78}$$

Inserting this expression into Eq. (3.17), the condition for the existence of a dust driven wind reduces to

$$\gamma(r_c) \, \frac{L_*}{L_{edd}} \gtrsim 1 \quad . \tag{3.79}$$

As by definition $\gamma \leq 1$, $L_* \geq L_{edd}$ follows as a necessary condition for a dust driven wind.

From Eq. (3.79) one further concludes i) that for a given value of $L_* > L_{edd}$, the degree of condensation γ has to exceed the minimum value

$$\gamma_{min}(r_c) = \frac{L_{edd}}{L_*} \quad , \tag{3.80}$$

and ii) that for a given value of γ the stellar luminosity L_* has to exceed the minimum value

$$L_{*,min} = \frac{L_{edd}}{\gamma(r_c)} \tag{3.81}$$

in order for a dust driven wind to develop. The r.h.s. of Eq. (3.81) is essentially determined by the stellar mass M_* and the mass loss rate $\dot{M}$. As $\dot{M}$ is fully determined by the stellar parameters L_*, M_*, T_* and $\{\epsilon_\ell\}$, thus, for given $\dot{M}$ and $\{\epsilon_\ell\}$, Eq. (3.81) yields a minimum mass loss rate

$$\dot{M}_{min} = \dot{M}_{min}(L_{*,min}, T_*) \tag{3.82}$$

defining a limit line in the HR-diagram which confines dust driven winds to those objects of mass M_* and abundances $\{\epsilon_\ell\}$ lying above this border line (cf. Fig. 10).

$\dot{M}_{min}$ depends strongly on the actual stellar gravitational field, i.e. on the mass of the considered object indicating that purely dust driven winds are expected only for low mass high luminosity stars situated at the right upper region of the HRD ([Dominik *et al.* 1990]). Furthermore, dust driven winds can exist only if a minimum amount of heavy elements condense into grains which by absorption and scattering of radiation gain sufficient momentum to be transferred to gas by effective collisional coupling. A quantitative discussion of these arguments shows that purely dust driven winds can exist only for objects having mass loss rates

$$\dot{M} > \begin{cases} 2\ldots3\cdot10^{-6}M_{\odot}\mathrm{yr}^{-1} & \text{(C-stars)} \\ 5\ldots8\cdot10^{-6}M_{\odot}\mathrm{yr}^{-1} & \text{(M-stars)} \end{cases} \tag{3.83}$$

respectively ([Gail and Sedlmayr 1987c]).

According to the observations (e.g. [Knapp 1985]), most C-stars fulfill this necessary condition, whereas only the most obscured M-stars exhibit such a high mass loss rate. For this reason, it must be concluded that in case of usual M-giants, the driving mechanism of their wind has to incorporate some additional ingredient (cf. our introductory remarks in Sect. 1 and the discussion of [Berruyer 1991]). Results of selfconsistent model calculations for C–stars are demonstrated and discussed in Sect. 6.

4 Chemistry of cool expanding shells

4.1 General considerations

While the outermost atmospheric layers of a star expand, both temperature and density decrease, thus, providing improved thermodynamic conditions for molecule formation in the wind, where along its cooling path monoatomic, diatomic, ... , polyatomic species are formed until finally favourable conditions for cluster formation and grain growth are met and dust formation sets on.

The chemical evolution during the outflow is described by a chemical reaction network which is basically determined by the adopted element abundances and the local temperature and density stratification and is controlled by various characteristic timescales introduced by the collision rates, the expansion velocity, the radiation field, the consumption of particular species due to condensation, etc.

The chemical reaction network is defined by the set of equations of continuity for the number densities n_i of species i which for spherically symmetric systems results in

$$\frac{\partial n_i}{\partial t} + 2n_i\frac{v}{r} + n_i\frac{\partial v}{\partial r} - Q_i = 0 \qquad i = 1,\ldots,I \tag{4.1}$$

with I being the total number of species considered, and Q_i the net source term due to chemical and photo processes. In principle, Q_i consists of four terms

$$Q_i = \Gamma_i^{ch} - \Lambda_i^{ch} + \Gamma_i^{ph} - \Lambda_i^{ph} \tag{4.2}$$

with

$$\Gamma_i^{ch} = \sum_j \Gamma_{ij}^{ch} \quad \text{sum of all kinetical gain rates} \tag{4.3a}$$

$$\Lambda_i^{ch} = \sum_j \Lambda_{ij}^{ch} \quad \text{sum of all kinetical loss rates} \tag{4.3b}$$

$$\Gamma_i^{ph} = \sum_j \Gamma_{ij}^{ph} \quad \text{sum of all gain rates of photo} - \text{processes} \tag{4.3c}$$

$$\Lambda_i^{ch} = \sum_j \Lambda_{ij}^{ch} \quad \text{sum of all loss rates of photo} - \text{processes} \tag{4.3d}$$

which contribute to species i.

The state of equilibrium of a chemical system is essentially determined by the relation between Q_i and the terms $\Gamma_{ij}^{ch}, \Lambda_{ij}^{ch}$, Γ_{ij}^{ph}, and Λ_{ij}^{ph} for the individual production and destruction processes contributing to the sum in Eq. (4.2). If Q_i is negligible compared to the individual source terms, Eq. (4.2) is approximately equivalent to the rate equations of an equilibrium system. Thus, one has to consider not only the total net rate Q_i but also the rates of the specific source processes in Eq. (4.3). For this discussion, however, it is sufficient to take into account only the most important reaction channel for kinetical reactions and photoreactions, respectively, which are defined by having timescales

$$\tau_i^{ch} = \min_j \left\{ \frac{n_i}{\Gamma_{ij}^{ch}}, \frac{n_i}{\Lambda_{ij}^{ch}} \right\} \tag{4.4a}$$

and

$$\tau_i^{ph} = \min_j \left\{ \frac{n_i}{\Gamma_{ij}^{ph}}, \frac{n_i}{\Lambda_{ij}^{ph}} \right\} \quad . \tag{4.4b}$$

These reaction timescales have to be compared with the corresponding hydrodynamical timescales

$$\tau_{dil} = \frac{r}{2v} \quad , \tag{4.5}$$

and

$$\tau_{acc} = \left(\frac{\partial v}{\partial r} \right)^{-1} \tag{4.6}$$

controlling the *dilution* of the gas by expansion and by *acceleration*, respectively.

By means of these timescales, the different states of equilibrium can be defined according to Table 1, where the various situations are listed using the reciprocal timescales which determine the importance of the different terms in the rate network (4.1):

In Table 1, the following cases have to be distinguished:

1. *Chemical Equilibrium* (CE): This case holds if all terms in the chemical network can be neglected besides the kinetical reaction rates. In CE every forward rate is in balance with its corresponding reverse reaction rate (*detailed balancing*), requiring

$$\Gamma_{ij}^{ch} = \Lambda_{ij}^{ch} \tag{4.7}$$

for all i and j.

Table 1: Different states of equilibrium: $\underbrace{a\ b\ \ldots} = \min\{a, b, \ldots\} \gg |a + b + \ldots|$.
All terms indicated by " $\ll$ " can be neglected against the terms inside the angular brackets.

	hydrodynamics			source terms		
	$\dot{n}_i/n_i$	$2v/r$	$\partial v/\partial r$	$\frac{1}{n_i}\sum_j \left(\Gamma_{ij}^{ch} - \Lambda_{ij}^{ch}\right)$	$\frac{1}{n_i}\sum_j \left(\Gamma_{ij}^{ph} - \Lambda_{ij}^{ph}\right)$	terms of Eq. (4.1)
1a	$\ll$	$\ll$	$\ll$	$\underbrace{\qquad\qquad}$	$\ll$ $\ll$	CE ($\rightarrow$ LTE)
1b	$\underbrace{\qquad\qquad\qquad\qquad}$			$\underbrace{\qquad\qquad}$	$\ll$ $\ll$	
2a	$\ll$	$\ll$	$\ll$	$\underbrace{\qquad\qquad\qquad\qquad\qquad\qquad}$		KE ($\rightarrow$ Non-LTE)
2b	$\underbrace{\qquad\qquad\qquad\qquad}$			$\underbrace{\qquad\qquad\qquad\qquad\qquad\qquad}$		
3	$\underbrace{\qquad\qquad\qquad\qquad\qquad\qquad\qquad\qquad}$				$\ll$ $\ll$	Non-CE
4	$\underbrace{\qquad\qquad\qquad\qquad\qquad\qquad\qquad\qquad\qquad\qquad\qquad\qquad}$					Non-KE
5	$\underbrace{\qquad\qquad\qquad\qquad}$			$\ll$ $\ll$	$\ll$ $\ll$	frozen chemistry
		τ_{dil}^{-1}	τ_{acc}^{-1}	$(\tau_i^{ch})^{-1}$	$(\tau_i^{ph})^{-1}$	timescales
				$\underbrace{\qquad\qquad\qquad\qquad\qquad\qquad}_{\tau_s^{-1} = Q_i/n_i}$		

CE requires in particular that effects due to velocity fields are small (1a) or balance for itself (1b) and that ionizing and dissociating photons can be neglected. In the context of radiative transfer, CE is equivalent to the assumption of LTE.

2. *Kinetical Equilibrium* (KE): In this case, which is defined analogously to non-LTE by vanishing net production rates for all chemical species

$$Q_i = 0 \qquad i = 1, \ldots, I \tag{4.8}$$

which expresses the fact that all chemical and photo-processes are in *statistical equilibrium.* Validity of the system (4.8) requires for Eq. (4.1) that either every change induced by the velocity field is negligible (case 2a) or at least that chemical processes and the velocity field decouple (case 2b).

3. *Non-CE:* This case is defined by negligible photorates but close coupling between the kinetical reactions and the hydrodynamics.

4. *Non-KE:* This is the most general situation where the full reaction network (4.1) comprising hydrodynamics, kinetical reactions and photoreactions has to be solved for obtaining the correct concentrations of the chemical species.

5. *Frozen chemistry:* Due to the dilution of the wind, the density decreases monotonically causing the chemical reaction rates (kinetical and photo–processes) to become negligibly small. Then, the evolution of the molecular concentrations is

solely determined by the hydrodynamical expansion of the flow. This case usually is addressed as "frozen chemistry".

Applying these criteria to the dust forming shells of late type giants shows that, depending on the specific situation, different states of equilibrium are to be expected:

If the shell chemistry is dominated by kinetic reactions, detailed balancing holds and consequently the assumption of chemical equilibrium (CE) is justified. Hence, CE is a reasonable assumption for all situations where UV-photons can be neglected and where the expansion velocities are sufficiently small for the local dilution timescale τ_{dil} to be large compared to the reaction rates involved. This is true for the innermost regions of the shells of chromosphere free C- and M-stars inside the sonic point. Outside the sonic point, the increasing supersonic velocity field causes a significant decrease of τ_{dil} which requires expansion effects to be taken into account, which in the extreme case of free expansion result in a frozen chemistry.

If chromospheres are present, in any case photoreactions dominate. Then, the entire shell departs from chemical equilibrium. Depending on the local dilution timescale τ_{dil}, in case of very small velocities (i.e. sufficiently inside the sonic point) *kinetic equilibrium* (KE) and in case of large velocities (i.e. in the expansion region) even Non-KE is expected.

4.2 The CO-molecule

Due to its exceptionally high bond energy ($E_{bond} \sim 11.09$ eV), the CO-molecule plays a decisive role with regard to the shell chemistry, because it is the first molecule to emerge in the flow and once it is formed, it can be dissociated only by rather high energetic photons.

Thus, in the *absence of dissociating UV-photons*, CO-formation in a circumstellar shell is a one-way process by which equal amounts of carbon and oxygen are consumed. This process proceeds until either carbon or oxygen nearly is exhausted. Under CE conditions, CO-formation takes place in the temperature regime between $T = 3000 - 2000$ K, i.e. well inside the sonic point. Hence, either carbon (in case of oxygen rich compositions: M-stars) or oxygen (in case of carbon rich compositions: C-stars) is blocked by CO in the outer parts of the shells, with the consequence that in the case of M-stars (C-stars) practically no additional carbon (oxygen) compounds can be formed. This important fact does not only determine the possible type of chemistry developing in such shells, but also restricts the number of possible condensating species and, thus, the chemical nature of the evolving dust components. This clear picture is considerably modified if UV-photons (as provided by chromospheres) capable to dissociate CO are present. In such cases, both for carbon *and* oxygen rich compositions always significant amounts of C-atoms, C^+-ions and oxides are found to coexist, which contaminate the above clear distinction and give rise to a complex carbon-oxygen chemistry (e.g. [Beck *et al.* 1992]). In these situations, the entire shell departs from CE and the full

KE or Non-KE reaction network has to be solved to obtain reliable molecular concentrations.

Irrespective of these considerations, in any case the outermost regions of the expanding shell will be affected by the interstellar radiation field which is capable even to dissociate CO, and which, therefore, has an important effect upon the chemical structure and the spectral appearance of the outermost regions of the shells whereas the central and inner parts are shielded by dust and molecular absorption (see e.g. [Mamon *et al.* 1988]). Such aspects, however, are beyond the scope of this paper.

4.3 The primary condensating species

Due to the expansion, the shell at some distance becomes cool enough for certain molecules to combine to clusters which then by further addition of molecules grow to macroscopic specimens (*dust grains*). In order to find out which molecules are most important for this initial step of cluster formation, usually three heuristic criteria are used to select the primary condensating molecules (see [Gail and Sedlmayr 1986], [Gail and Sedlmayr 1987a]):

i) *The clustering molecules must not be blocked by high bond energies.* Being a chemical process, cluster formation involves reactive species. For this reason, all molecules having a bond energy which is larger than the reaction energy required for cluster formation behave practically inert and, thus, cannot participate in the condensation process.

ii) *The resulting clusters have to be high temperature condensates.* This requirement is motivated by the observations which suggest a temperature range from 1300 to 700 K for the dust formation region.

iii) *The clustering molecules have to be abundant species in the gas phase.* This criterion is motivated by the observational fact that many circumstellar dust shells show large optical depths caused by dust absorption. Then the deduced large dust to gas ratios can only be explained if abundant heavy elements contribute to the condensation process.

Applying these criteria to dust producing shells, only a rather limited number of species should be involved in the primary condensation process which, in cases where ionizing and dissociating photons are absent, are found to be

- SiO, MgO, MgS and Fe
  for oxygen rich compositions (M-stars without chromospheres),

- C_2H_2, C_2H, MgS, SiC and Fe
  for carbon rich compositions (C-stars),

respectively. Then only neutral species contribute to cluster formation.

In situations contaminated by ionizing and dissociating UV-photons, the problem of primary condensates is much more difficult, not only due to a considerably larger variety of possible species (ions etc.) involved but also with regard to the condensation process itself, which then has to be considered as heterogeneous nucleation which, in principle, requires to solve a chemical rate network (including ion–neutral reactions) far into the nucleation regime (see [Sedlmayr 1994]). For these reasons, until now no generally accepted treatment of cluster formation in shells where UV-photons determine the chemistry has been developed.

5 Dust formation

5.1 General considerations

From a microscopic point of view, dust formation can be considered as the extension of the gas phase chemistry into the region of clusters and macroscopic dust grains. The most general description of this process is a network of chemical rate equations containing all relevant molecules, clusters, and grains, and all important reactions. However, since the complexity of such a network increases exponentially with the size of the treated molecules, a description on this general level is completely impractical. Fortunately, since the properties of molecules and macroscopic dust grains are quite different, the continuous grain formation process usually can be split into two parts where different descriptions are appropriate (cf. [Gail and Sedlmayr 1988], [Sedlmayr 1994]).

5.1.1 The molecular domain

The low-size regime of the chemical network describes the concentrations of small molecules consisting of only a few atoms. At these sizes, the properties of each kind of molecules are very specific. The reaction rates in this domain cover a range of many orders of magnitude. In particular, in a chain of reactions, the times required for two subsequent steps may be very different and each individual molecule has its special properties and reactions. Since the rate of formation of dust grains, which is the most critical quantity in any theory of dust formation, is determined by such chains, a chemical description on the basis of a network, if possible, will provide the best results.

5.1.2 The macroscopic particle domain

The description of reactions between macroscopic dust grains and molecules is (to some extent) more simple than the treatment of molecule–molecule reactions, since the properties of macroscopic particles become less dependent on the size of the particle as the size increases. Very often the relaxation time towards internal thermal equilibrium within the grains is much smaller than the characteristic time in which the conditions in the gas change considerably, or in which the composition and the size of the grains are altered. A grain then has an internal temperature T_d governing the distribution of energy in the different degrees of freedom, and the spontaneous processes like the emission of a molecule become independent of the properties of the surrounding gas. Furthermore, for a given chemical composition of the grain, the properties of the surface are independent of its size. Every unit surface area has a certain amount of possible sites where reactions with admolecules from the gas can occur. Thus, the rates of most processes simply become proportional to the surface area of the grain. This property allows for a very simple and efficient calculation of macroscopic particle growth (cf. Sect. 5.3).

5.2 Calculation of the nucleation rate

The calculation of the nucleation rate has been treated in a variety of different approximations and with several different basic assumptions. Fig. 3 gives an overview of the different possibilities.

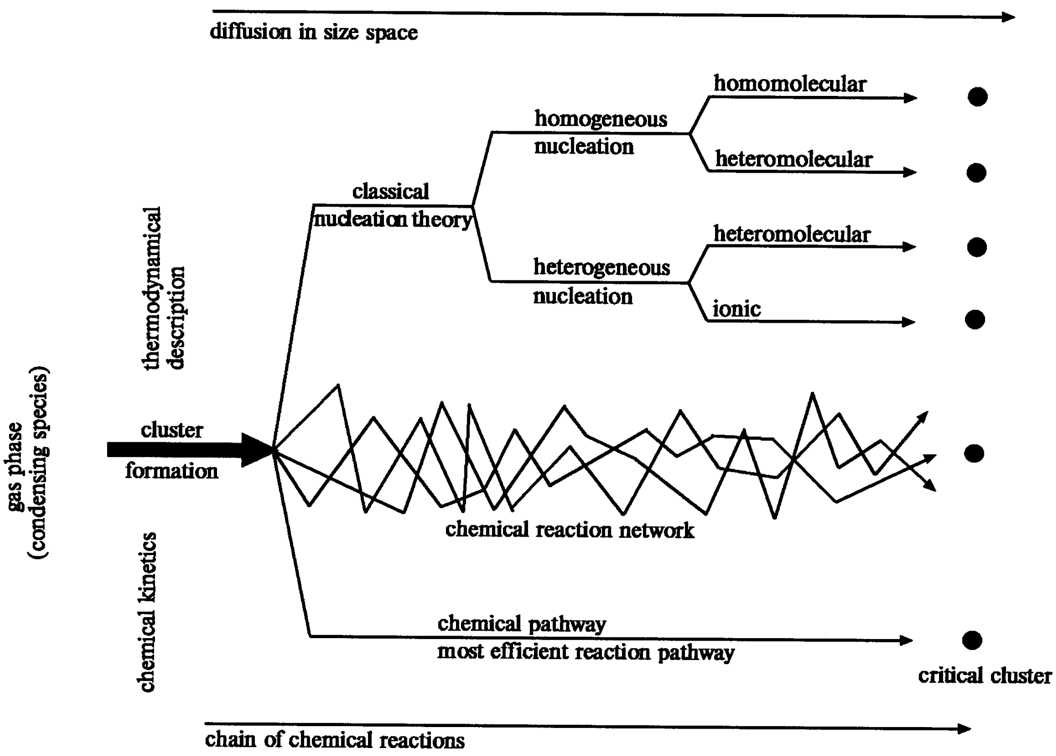

Fig. 3. The different possibilities for the description of the nucleation process as discussed in the text (adopted from [Sedlmayr 1994]).

As discussed above, the most general description of the nucleation process is the solution of the relevant network of chemical equations. If the basic dust forming chemistry is in fact a complex network of reactions, only the solution of the complete network yields correct results. However, the complete network is usually unknown. In astrophysical context, only [Rawlings and Williams 1989] (in the case of a nova and under the assumption that hydrocarbon chain molecules lead to dust formation) and [Keller 1987], [Frenklach and Feigelson 1989], and [Cherchneff *et al.* 1991] (in the case of PAH formation in stellar winds around carbon-rich stars) have attempted this way. Since the solution of the rate equations is involved, this approach has not been coupled with hydrodynamic and radiative transfer equations so far, which of course is critical for the description of a dust driven wind. Other descriptions of dust formation, therefore, deal with an approximate treatment of the chemistry relevant for nucleation. These descriptions either are based on a thermodynamical approach (*classical nucleation theory*) or on the discussion of a selected chemical pathway. Since classical nucleation theory can be viewed as a pathway description along a particular coordinate in the cluster size space, in the following, we will treat the two approaches together.

The basic idea behind both descriptions is that the nucleation process of a grain proceeds along a *chemical pathway.* This concept requires the selection of the most efficient one-dimensional sequence of reactions from the network, thus defining a *chain* of molecules. Each chain molecule (except for the starting point of the chain) is linked by two reactions of the pathway: One reaction transforms the molecule into the next chain molecule, the other into the previous one. A schematic sketch of such a pathway is shown in Fig. 4. The most simple example is given by homogeneous classical nucleation theory in which all considered clusters are polymerisations of only one kind of monomer. An example is the formation of water droplets out of a supersaturated pure water vapor. This kind of nucleation is called *homomolecular* (since growth is due to only one kind of molecule), *homogeneous* (since all clusters and grains are homogeneously composed of a single monomer) *nucleation.* However, generalizations of this concept have been made. [Gail and Sedlmayr 1988] describe *heteromolecular homogeneous nucleation* in which the grains consist of only one special monomer but the growth is due to molecules containing one or several monomers. Kozasa and Hasegawa (1987) worked with *heteromolecular heterogeneous nucleation* where the grains are also homogeneous, but since the monomer of the considered condensates does not exist in the gas phase, a certain constant *sequence* of reactions is assumed to build the monomer in the grain. In the reaction chains describing the formation of PAH's ([Keller 1987], [Gail and Sedlmayr 1987a], [Frenklach and Feigelson 1989], [Cherchneff *et al.* 1991]), not every reaction directly contributes to the growth. After every growth step (e.g. addition of C_2H_2), a hydrogen abstraction reaction is required in order to create a new radical site which in turn allows for a further growth reaction.

In order to select a certain pathway independent of other parts of the chemical network, it is essential that the pathway is *isolated* in the sense that all relevant reactions proceed *along* the pathway. This situation is indicated in Fig. 4 by the

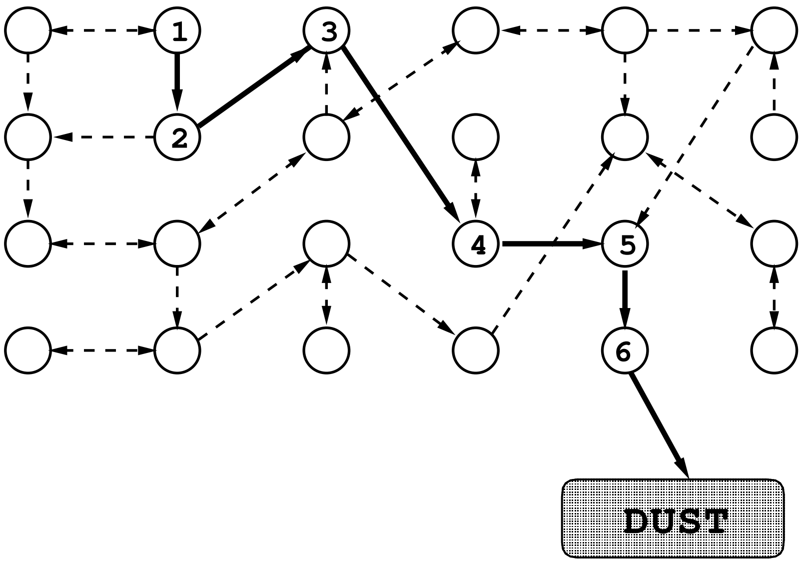

Fig. 4. Schematic sketch of a chemical network with a highlighted pathway to dust formation (after [Goeres 1993]).

thickness of the arrows. The reactions along the chain are much more important than reactions of chain molecules with other molecules. In this case, the concentrations of the chain molecules are determined by chain processes only. The flux through the chain which equals the nucleation rate can then be calculated in a rather simple way. Though not always explicitly stated, the assumption that the chain is isolated is implicitly used in all nucleation theories up to now applied in model calculations of stellar winds, except for the network approaches discussed above.

5.2.1 Calculation of the flux through a chain

We denote the subsequent molecules in the chain by the subscript i. The flux through the chain from molecule i to $i+1$ is then given by:

$$J_{i+1} = n_i \beta_i - n_{i+1} \gamma_{i+1} \qquad i \geq 1, \tag{5.1}$$

where n_i, n_{i+1} denote the number densities of the chain molecules i and $i+1$, respectively. β_i and γ_{i+1} denote the reaction rates per molecule for step $i \rightarrow i+1$ and $i+1 \rightarrow i$, respectively, each given by the product of the number density of the reaction partner and a rate coefficient.

In the situation of a dust driven wind, the chemical time scales are usually much smaller than the time scale for the changes in hydrodynamical quantities like ρ, T

(cf. [Gail and Sedlmayr 1988]). Therefore, the densities n_i become independent of time. All important reactions occur along the chain. This directly implies that the flux through the chain becomes independent of i, at least for the initial steps of the chain. Thus

$$J_i = J^s \qquad i = 1, \dots, I+1, \tag{5.2}$$

where J^s is the *starting nucleation flux* and I is some large number leading into the growth regime, but which is still small enough to ensure that n_{I+1} still is independent of time. Eqs. (5.2) allow to eliminate explicitly the densities n_2, ..., n_I in order to calculate the stationary flux J^s

$$J^s = \frac{n_1\beta_1}{1 + \frac{\gamma_2}{\beta_2} + \frac{\gamma_2\gamma_3}{\beta_2\beta_3} + \dots + \frac{\gamma_2\gamma_3\dots\gamma_I}{\beta_2\beta_3\dots\beta_I}} \quad . \tag{5.3}$$

The denominator in Eq. (5.3) contains products of γ_i/β_i which are the branching ratios for a molecule i, either to move forward or backward in the chain. In a supersaturated gas, where the solid is stable, the ratio γ_i/β_i becomes very small for large clusters having already the structure of the stable condensate (growth much more probable than decay), while it may be larger than unity for small molecules (decay more probable than growth). Thus, the sum will be dominated by a certain term containing the larger than one factors γ_i/β_i but not the smaller than one factors. The last factor in that particular term will be of the order of $\gamma_{i^*}/\beta_{i^*} \simeq 1$. The corresponding molecule i^* is called the *critical cluster* which grows and shrinks with nearly equal probability (see also [Goeres 1993]). The flux J^s in the chain is, therefore, essentially determined by the reactions *below* the critical cluster:

$$J^s \approx n_1\beta_1 \frac{\beta_2\beta_3\dots\beta_{i^*}}{\gamma_2\gamma_3\dots\gamma_{i^*}} \quad . \tag{5.4}$$

It is clear that the main practical difficulties in the application of Eq. (5.3) or (5.4) are (i) the determination of the most effective reaction chain that leads to dust formation, and, (ii) the knowledge of all reaction rates along this chain up to the critical cluster. Up to now, this is only possible in quite specific situations such as the formation of polycyclic hydrocarbons in a carbon-rich chemistry.

The expression for the nucleation flux is considerably simplified, if the growth and shrink rates β_i, γ_i are the same as in the chemical equilibrium state corresponding to the density n_1 of the chain starting molecule. This is for example true when the growth reactions are due to only a few molecules which are in fact in equilibrium with n_1. Especially, in case of classical homogeneous nucleation, cluster growth and destruction are simply due to condensation and evaporation of the monomer, which by definition is the first chain molecule.

We denote all quantities in chemical equilibrium with a circle above the symbol. Under the assumptions $n_1 = n_1^\circ$, $\beta_i = \beta_i^\circ$, $\gamma_i = \gamma_i^\circ$ it is possible to apply the *Milne relations*

$$\frac{\beta_i^\circ}{\gamma_{i+1}^\circ} = \frac{n_{i+1}^\circ}{n_i^\circ} \qquad i \geq 1 \quad . \tag{5.5}$$

Then, Eq. (5.3) may simply be written as

$$J^s = \left\{ \sum_{i=1}^{I} \frac{1}{n_i^\circ \beta_i^\circ} \right\}^{-1} \quad . \tag{5.6}$$

Since the equilibrium densities of the different chain molecules usually differ by orders of magnitude, J^s is essentially determined by the minimum value of $n_i^\circ \beta_i^\circ$, $i = 1 \ldots I$. Thus Eq. (5.6) reduces to

$$J^s \simeq n_*^\circ \beta_*^\circ \quad , \tag{5.7}$$

where the cluster $i = i^*$ is the critical cluster. The simple interpretation of Eq. (5.7) is, that all reactions in the chain before the critical cluster are fast enough to almost establish the equilibrium densities up to $i = i^*$. Since i^* is the last cluster with a relevant destruction probability, every reaction $i^* \rightarrow i^* + 1$ supplies one growing nucleus for dust formation.

Eq. (5.6) opens another possibility for the calculation of J^s if the conditions are appropriate. Besides the forward reaction rates β_i°, Eq. (5.6) only requires the knowledge of the thermodynamical functions of the chain molecules, in particular the Gibbs free enthalpy of formation ΔG_i in order to calculate the equilibrium densities n_i°. For example, in the standard case of classical homogeneous nucleation theory, the subscript i counts the number of monomers in a cluster having equilibrium density

$$n_i^\circ = (n_1^\circ)^i \exp\left\{ -\frac{\Delta G_i}{kT} \right\} \quad . \tag{5.8}$$

However, the determination of ΔG_i for all contributing molecules and clusters is very difficult and up to now only possible in special situations. The most prominent example again is the formation of PAHs, where the thermodynamic functions can be calculated with sufficient accuracy by group additivity rules (cf. [Benson 1976]). For the application of this method to grain formation see [Keller 1987] and the review of [Frenklach and Feigelson 1989].

The most widely applied approach for the determination of nucleation rates is the extrapolation of the thermodynamic properties of the bulk material down to clusters and even molecules. The reduced bond energy of monomers near the surface of a cluster is accounted for by introducing the concept of a surface tension (see the review by [Feder *et al.* 1966]), which is either assumed to be constant, or is parametrised in order to simulate the decrease of the surface tension with decreasing cluster size (cf. [Draine and Salpeter 1977]). Although this concept leads to reasonable results for clusters not too small, it certainly breaks down for molecules. As the critical cluster size in astrophysics usually is only few molecules, this surface tension concept has legitimately been criticized in the past (e.g. [Donn and Nuth 1985]) and is the main reason for the reservations against the application of classical nucleation theory in the context of astrophysical grain formation. However, [Hale *et al.* 1989] have shown that the results of laboratory nucleation experiments may at least in some cases be fitted by a law similar to the formulae of the classical nucleation theory ([Hale 1986]). As long as thermodynamical data for astrophysical clusters are not available, one certainly has to live with this type of approximation as a crude description for the real processes taking place.

Another reason why the surface tension approach is so popular is, that it provides an analytical expression for the Gibbs energy of formation as a function of cluster size and temperature. Since the flux through an isolated chain is essentially determined by the cluster with minimum equilibrium concentration (Eq. (5.7)), the critical cluster can be derived directly from the analytical determination of the minimum of $n_1^i \exp\left\{-\frac{\Delta G(T,i)}{kT}\right\}$, interpreted as a continuous function of i. In case that temperature and particle densities in the gas are simple functions of time, the whole problem of nucleation and dust growth may be solved analytically (e.g. [Draine and Salpeter 1977], [Yamamoto and Hasegawa 1977]). However, due to the complex non-linear interaction between dust formation and hydrodynamics, especially in dust driven winds, a numerical treatment seems to be more appropriate.

5.3 The growth of dust grains

When a cluster surmounts the condensation barrier indicated by the critical cluster, it becomes thermodynamically stable and will grow continuously. When it becomes sufficiently large in order to be treated as a macroscopic particle having a well defined internal temperature and broad absorption characteristics instead of lines and bands, we call this particle a dust grain. Particles with this properties usually must consist of at least about 100 atoms which corresponds to a cluster size of about 10^{-7} cm. As in dust driven winds the time scale for chemical reactions are considerably smaller than those governing the hydrodynamics, this limiting size is reached quickly. Thus, we assume that each cluster above the critical cluster almost instantaneously reaches the *limiting radius* a_ℓ. We denote the rate of formation of clusters with size a_ℓ by J_ℓ and assume that it is equal to J^s.

From there the grain may grow in a variety of ways. Fig. 5 gives an overview over the possible growth mechanisms. The most simple is homogeneous growth of a homogeneous grain, where in each growth process one or several identical monomers are added to the grain.

The type of the crystal structure formed is very much dependent on the relation

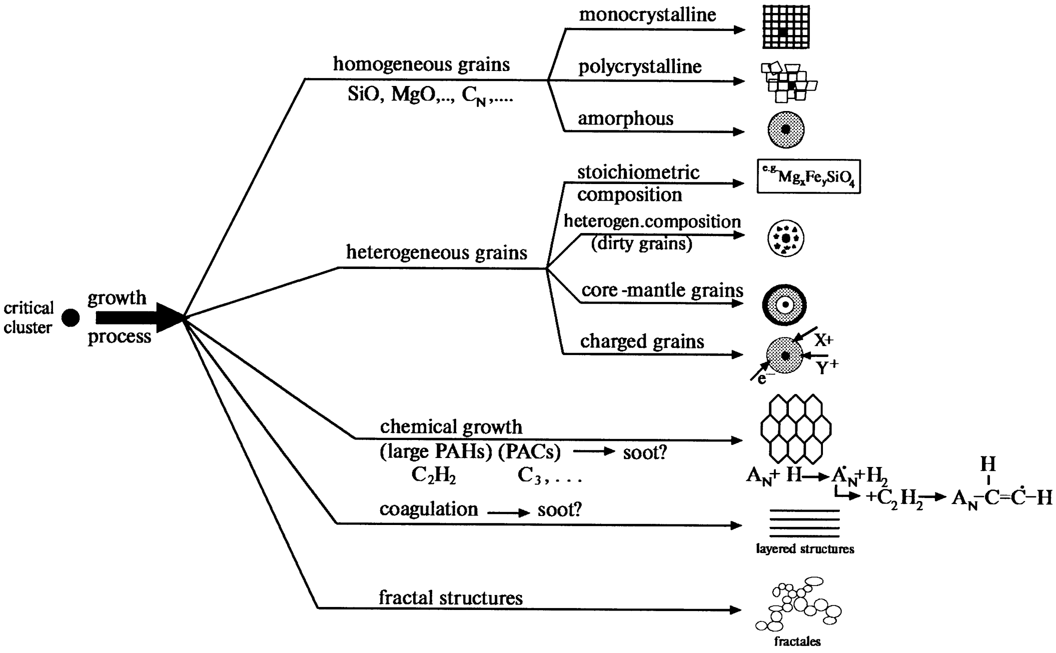

Fig. 5. The different possibilities for the growth of dust grains and the resulting structure (adopted from [Sedlmayr 1994]).

between the growth time scale which is given by the flux of material condensing onto the grain, and the time scale for an admolecule to reach its energetically most favourable site by hopping processes on the surface of the grain ([Gail and Sedlmayr 1984]). If each molecule has always enough time to reach its energetically most favourable site before it is coated by other molecules, the grain will be ordered on large scales resulting in a *monocrystalline structure*. If the admolecule has only enough time to reach a locally favourable site, the crystal structure will be locally ordered, which is usually referred to as *polycrystalline structure*. Finally, if the growth is much faster than the hopping time scale, an *amorphous grain* will form.

The next possibility is the growth of a grain by a variety of molecules. The resulting grain still might develop a homogeneous structure if the same sequence of growth steps is followed all the time. If this is not the case, the grain becomes heterogeneous and the chemical composition is a function of the position in the grain. If the resulting grain structure is spherically symmetric, such grains are usually referred to as *core-mantle grains*.

A further possible growth mechanism is coagulation of grains. This process might have some significance for the formation of graphite like structures on the basis of PAHs, but most probably it is of no significance in the winds of red giants ([Dominik *et al.* 1989]).

In the following, we describe an efficient method for the calculation of grain growth applicable under most circumstances discussed above.

5.3.1 The moment equations for the growth of dust grains

A very important information about the dust component is contained in the *size distribution function* (cf. Sect. 3.2.3)

$$f(a)da \qquad a \geq a_\ell \quad , \tag{5.9}$$

which counts the local number density of dust grains in the grain radius interval $(a, a+da)$. The size distribution has a lower limit for the size a since only particles with a larger than a_ℓ are considered to be grains.

The growth of dust grains is generally due to reactions of the type

$$G + M \rightarrow G'(+M') \quad , \tag{5.10}$$

where a dust grain G and a molecule M react and the result is a changed dust grain G', and perhaps another molecule M'. As far a the size of the particle is considered, the net effect of such a reaction can be described by a *change in volume* of the grain. The volume V_i attributed to every reaction is defined to be the average volume the added or abstracted molecule has in the crystal structure actually formed on the grain surface. Generally this volume may be different at different temperatures.

The rate of reactions of a dust grain with a certain kind of molecule can be written as

$$R_i = A\omega_i \quad , \tag{5.11}$$

where A is the surface area of the grain and ω_i is the reaction frequency per unit surface area. The subscript i distinguishes different reactions. ω_i can be written as

$$\omega_i = n_i v_i \alpha_i \quad , \tag{5.12}$$

where n_i is the number density of the molecule responsible for reaction i, v_i is the mean relative velocity between the grain and the molecules and α_i denotes the probability that a collision between grain and molecule leads to a reaction. If the local velocity distribution of the molecule is Maxwellian, and the (spherical) grain is drifting with a velocity v_D relative to the gas, v_i is given by

$$v_i = \sqrt{\frac{kT}{8\pi m_i}} \left[\frac{\sqrt{\pi}}{s_i}(2s_i^2 + 1)\phi(s_i) + s_i exp(-s_i^2) \right]$$

and (5.13)

$$s_i = v_D\sqrt{\frac{m_i}{2kT}} \quad , \tag{5.14}$$

where m_i is the mass of the molecule responsible for reaction i and ϕ(s) is the error function.

Each reaction shifts the size of a grain and therefore changes the value of the size distribution function. The total rate for $df(a,t)/dt$ can be obtained from the sum over all contributing processes:

$$\begin{aligned} \frac{d}{dt}f(a,t) &= \sum_i f(a_{\rm ref}(a,V_i),t)\,A(a_{\rm ref}(a,V_i))\,\omega_i \\ &- \sum_i f(a,t)\,A(a)\,\omega_i && (5.15) \\ & && (5.16) \end{aligned}$$

with

$$a_{\rm ref}(a,V_i) = \left(a^3 - 3V_i/(4\pi)\right)^{1/3} \tag{5.17}$$

and

$$A(a) = 4\pi a^2 \tag{5.18}$$

under the assumption of spherical grains.

If the reaction frequency is dependent on the grain size (due to, for example, a size dependence of the drift velocity or of the grain temperature) the growth of each grain has to be treated individually. If, on the other hand, ω_i does not depend on the grain size (e.g. if all drift velocities are equal or at least small compared to the thermal motions of the molecules), the complete growth process can be described by a simple set of ordinary differential equations for moments of the size distribution.

The moments of the size distribution function, first introduced in Eq. (3.64), are defined by

$$K_j(t) = \int_{a_\ell}^{\infty} da a^j f(a,t) \quad j = 0,1,\ldots \quad , \tag{5.19}$$

Thus, many important quantities can be derived from the knowledge of the moments only, e.g.:
number of dust grains per cm^3:

$$n_d = K_0 \tag{5.20}$$

and mean values for the powers of the particle radius:

$$\langle a^j \rangle = \frac{K_j}{K_0} \quad . \tag{5.21}$$

For reason of simplicity it is often advantageous to normalize the moments and the size distribution by the size of a volume flowing with the grains in order to get rid of volume related terms. We use the total number density of hydrogen nuclei $n_{<H>} \approx n_H + 2n_{H_2}$ for this normalization and denote all quantities subjected to this normalization by a hat ˆ above the corresponding symbols:

$$\hat{f}(a,t) = f(a,t)/n_{<H>}; \quad \hat{J}_\ell(t) = J_\ell(t)/n_{<H>}; \quad \hat{K}_j(t) = K_j(t)/n_{<H>} \quad . \tag{5.22}$$

With the assumption that the flux of grains through the lower boundary a_ℓ is given by the known nucleation rate $\hat{J}_\ell$, the following set of equations can be calculated straight forward (multiplying Eq. (5.15) by a^j and integrating from a_ℓ to infinity, for details see [Gail and Sedlmayr 1988], [Dominik 1992], [Dominik *et al.* 1993]):

$$\frac{d}{dt}K_j = J_\ell a_\ell^j + j\xi K_{j-1} \qquad j = 0, 1, \ldots \quad , \tag{5.23}$$

where the quantity

$$\xi = \sum_i \omega_i V_i \tag{5.24}$$

is the growth velocity of the grain radii in cms^{-1}.

These equations provide a very simple and effective way of calculating the moments of the size distribution function.

By definition, the moments carry only information about mean values of the size distribution function. For some purposes, however, such as the calculation of exact optical properties of the dust component, the complete distribution must be provided - a task that generally requires the knowledge of an infinite number of moments. Fortunately, in the special case of dust formation in a stellar wind this is not necessary. Since, at a given instant, all dust grains either grow or shrink, it is sufficient to consider the number of dust grains smaller than a given size $\tilde{a}$ ([Dominik *et al.* 1993]). If the formation time of grain nuclei having size $\tilde{a}$ at time t, is denoted by $t_{\mathrm{nuk}}(\tilde{a})$, $\tilde{a}$ is immediately given by

$$\tilde{a} = a_\ell + \int_{t_{\mathrm{nuk}}(\tilde{a})}^{t} dt' \xi(t') \quad . \tag{5.25}$$

All grains smaller than $\tilde{a}$ must have formed later than $t_{\mathrm{nuk}}(\tilde{a})$. Its number density, therefore, results to

$$\int_{a_\ell}^{\tilde{a}} \hat{f}(a,t) da = \int_{t_{\mathrm{nuk}}(\tilde{a})}^{t} dt' \hat{J}_\ell(t') \quad . \tag{5.26}$$

Differentiating Eq. (5.26) with respect to $t_{\mathrm{nuk}}(\tilde{a})$ yields

$$\hat{f}(\tilde{a},t) = \hat{J}_\ell(t_{\rm nuk}(\tilde{a})) \left(\frac{da}{dt}\right)^{-1}_{t_{\rm nuk}(\tilde{a})} = \left(\frac{\hat{J}_\ell}{\xi}\right)_{t_{\rm nuk}(\tilde{a})} \quad . \tag{5.27}$$

Since the growth velocity ξ is the same for all dust grains, growth can be viewed as a uniform translation of the particle size distribution function through the grain radius space. Therefore it is sufficient to follow the evolution of a single particle in order to establish the relation (5.25) for all dust grains, and the size distribution function at every instant is given by the solution of the following set of equations ([Gauger *et al.* 1990]).

$$\frac{da_{\rm max}(t)}{dt} = \xi \tag{5.28}$$

$$g(a_{\rm max}(t)) = \left(\frac{\hat{J}_\ell}{\xi}\right)_t \tag{5.29}$$

$$\hat{f}(a,t) = g(a_{\rm max}(t) - a + a_\ell) \quad , \tag{5.30}$$

where $a_{\rm max}(t)$ is the maximum grain radius at time t.

Eqs. (5.28)-(5.30) are sufficient to calculate all relevant properties of homogeneous dust in the case of monotonic growth. The generalization to oscillating situations with intermittent evaporation is straight forward. Furthermore, the independence of the growth processes of the grain size implies, that all grains have the same structure as a function of depth below the grain surface. The above scheme can thus also be used to keep track of a changing chemical composition, crystal structure, etc. inside the dust grains and therefore of the formation of layered dust particles. If we consider suitable parameters Ψ_i which characterize the chemical composition or any other structural quantity of interest, we may define the functions

$$\psi_i(a_{\rm max}(t)) = \Psi_i(t) \quad . \tag{5.31}$$

The internal structure of a grain of size $a(t)$ can then be described in terms of Ψ_i as a function of distance ℓ, $\ell \le a(t)$ from the center of the grain. By similar arguments as above the structure can be shown to be

$$\Psi_i(\ell, a(t), t) = \psi_i(a_{\rm max} - a(t) + \ell) \qquad a_\ell < \ell \le a(t) \ , \tag{5.32}$$

which allows to calculate the internal chemical structure of heterogeneous grains along its trajectory in the wind ([Dominik 1992], [Dominik *et al.* 1993]).

6 Models of dust driven winds

6.1 Overview

The problem of a dust driven wind, which has been formulated in the Sections 3–5, has been addressed in the past by several authors adopting different levels of approximations and focusing on different aspects of the problem.

The first quantitative treatment of dust driven winds is due to [Salpeter 1974a; Salpeter 1974b] who discussed analytical solutions of the gas-dust system in the wind and their dependence upon the luminosity of the star. [Kwok 1975] assumed instantaneous nucleation at a critical temperature in an adiabatic flow, identified this point with the sonic point of the wind equation and calculated the further growth of the dust grains including effects of drift and sputtering. [Lucy 1976] made a simple assumption of instantaneous nucleation and growth of the dust grains at some point, but also introduced his approximation for a semi-analytical treatment of the radiative transfer (see Appendix). [Deguchi 1980] used the analytical expressions for dust formation by [Salpeter 1977] and by [Yamamoto and Hasegawa 1977] in order to calculate numerical models of the complete wind region. A similar approach has been followed by [Kozasa *et al.* 1984]. [Menietti and Fix 1978] concentrated on the produced spectra of a dust driven wind, especially on the 10 μm silicate feature. [Tielens 1983] also used a simple assumption for grain formation. He focused in considerable detail on the treatment of heating of the wind by friction between drifting grains and gas and cooling due to H_2O emission.

[Gail and Sedlmayr 1985] introduced chemical equilibrium calculations and their moment method to dust driven winds and calculated the first selfconsistent model including equilibrium chemistry, time dependent treatment of dust formation and growth and a treatment of radiative transfer in the Lucy approximation ([Gail and Sedlmayr 1987b]). These calculations where extended by [Dominik *et al.* 1990] for a large range of stellar parameters. Recently, [Winters *et al.* 1994] have included detailed radiative transfer and calculated spectra. In the next section we will discuss one of these models in some detail.

6.2 A selfconsistent model for a dust driven wind

The model calculations by [Winters *et al.* 1994] were carried through for carbon stars with solar abundances except for an enrichment in carbon relative to oxygen. In this case, element abundances of the model are given by a single parameter, $\varepsilon_C/\varepsilon_O$. The model is then completely described by a set of four independent parameters (see Sect. 1). Since the radiative transfer is calculated in detail, the photospheric temperature is a result, thus M_*, L_*, $\dot{M}$, and $\{\epsilon_\ell\}$ are the fundamental stellar parameters in this case.

The model calculations basically solve the complete set of equations described in Sects. 3–5, with the following assumptions and simplifications:

1. Gas and dust are assumed to be strictly momentum coupled. As discussed in

Sect. 3.2.1 this is a reasonable assumption for small particles – it breaks down for very large grains.

2. Gas and dust temperatures are calculated from the assumption of radiative equilibrium.
3. The chemical composition is calculated from chemical equilibrium. For the actual calculation a reduced set of molecules: H_2, CO, C_2, C_2H, C_2H_2 ,C_3, C_3H is considered, which is sufficient for an accuracy of the molecule concentrations of about 5%.
4. The nucleation rate is calculated from classical nucleation theory in the modifications of [Draine and Salpeter 1977] and [Gail *et al.* 1984] applied to carbon with a value for the surface tension of 1400 erg cm^{-2}. The material growing onto these nuclei is pure amorphous carbon.
5. The gas opacities are Rosseland mean opacities. The dust opacities are calculated from Mie theory under full treatment of the local dust size distribution function (see Sect. 3.2.3). The optical properties of the dust material are those for amorphous carbon given by [Maron 1990].

The model parameters were adjusted to fit the emergent spectrum of the well known carbon star IRC+10216 at luminosity maximum (see Fig. 9). The model parameters for the best fit are $M_* = 0.7M_{\odot}$, $L_* = 2.4{\cdot}10^4 L_{\odot}$, $\dot{M} = 8{\cdot}10^{-5}M_{\odot}\mathrm{yr}^{-1}$, and an abundance ratio of carbon to oxygen $\varepsilon_C/\varepsilon_O = 1.4$.

The radial structure of this model is shown in Fig. 6. The onset of condensation is located around $1.4R_0$, where $R_0 = 9.25 \cdot 10^{13}$cm is approximately the photospheric radius of the star (see [Winters *et al.* 1994]). [1] The fact that dust forms already quite close to the star is very important for a dust driven wind. In a static atmosphere the density decreases exponentially near the photosphere, as can be seen from the plot of ρ in Fig. 6a. In order to drive effectively a massive wind, the wind formation mechanism must operate quite close to the star. High densities are also required for effective dust formation to occur and this again is realized close to the star. However, this restriction can be softened, if the atmosphere is already extended by a different wind-supporting process.

The onset of condensation is reflected in Fig. 6a by a steep increase of the flux mean of the dust extinction. This flux mean is directly related to the radiative acceleration of the wind, since the dust grains transfer their momentum by collisions to the gas (instantaneously in this calculation, see Eqs. (3.7)). The resulting acceleration α, measured in units of the local gravitational acceleration, is plotted in Fig. 6b. α rises rapidly and at about $4\mathrm{R}_0$ reaches a maximum value of about 7.

[1] In the following, the symbol $R_{\circ}$ denotes the stellar radius of the starting model which is defined by Eq. (A.25) in Lucy's grey approximation ($\kappa_J = \kappa_B$). The stellar radius of the converged model presented here, defined by (3.57) $L_* = 4\pi R_*^2 \sigma T_*^4$ and the requirement (A.21) $T(R_*) = T_*$ results in $R_* = 0.96R_{\circ} = 8.88 \cdot 10^{13}$ cm (cf. Appendix of [Winters *et al.* 1994]).

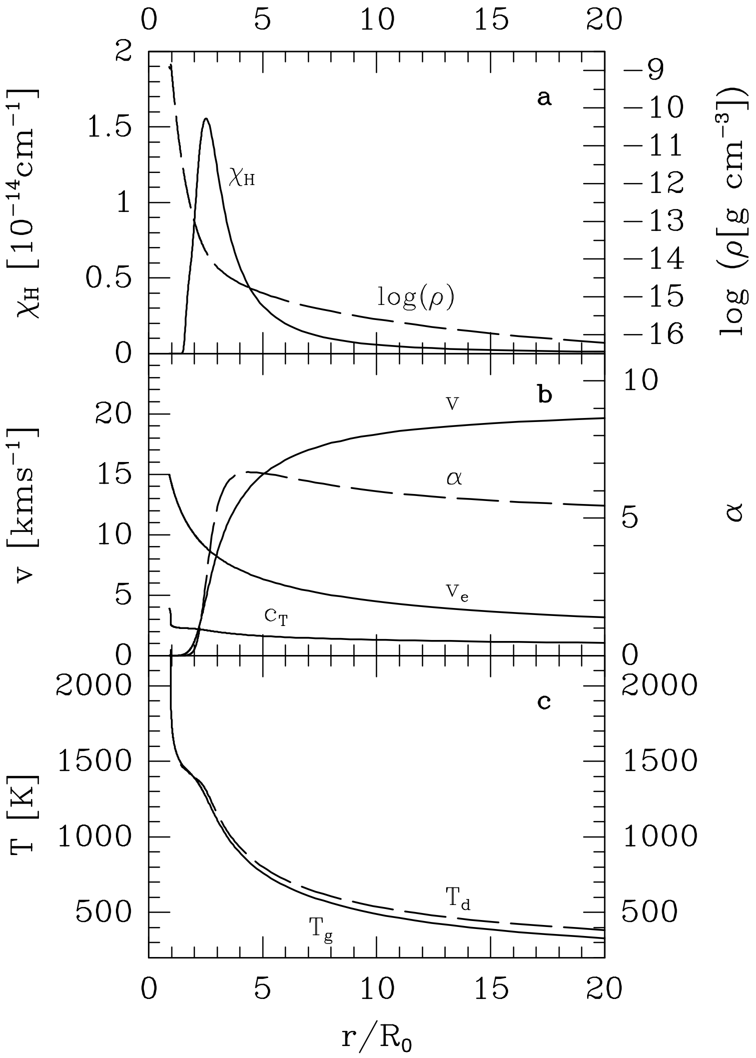

Fig. 6. Radial structure of the model discussed in the text. a) flux mean extinction coefficient χ_H of the dust component, mass density ρ. b) hydrodynamic velocity v, local sound speed c_T, local escape velocity v_e, and radiative acceleration α in units of the gravitational acceleration. c) gas temperature T_g and dust temperature T_d (after [Winters *et al.* 1994]).

Due to this acceleration, the static structure of the atmosphere is changed and a wind develops: the wind velocity v increases and the course of ρ changes gradually from an exponential decrease to a r^{-2} decrease. At $r = r_c = 2.2R_0$, the wind goes through the subsonic-supersonic transition (cf. definition by Eqs. (3.13) and

(3.14)). Note that at this position α is only about 0.75, so radiative acceleration does not yet balance the gravitation and the pressure gradient is still an important factor. Slightly outside the sonic point the radiative acceleration completely dominates. Around $r = 3R_0$, v crosses the line of the local escape velocity and the wind becomes gravitationally unbound. However, the acceleration is still active and the wind reaches its final velocity of $20.7\,\mathrm{kms}^{-1}$ near $r = 20R_0$.

Immediately after the onset of dust formation, the temperatures of dust and gas become different (Fig. 6c). The dust temperature everywhere exceeds the gas temperature – the dust shows a positive greenhouse effect. The maximum value of the difference $T_d - T_g$ in this model is about 50 K, and is mainly a function of the optical thickness of the dust envelope. It can be much larger in more optically thin envelopes. Inside the dust shell, the thermal emission from grains produces a pronounced backwarming effect which leads to a temperature plateau just inside of the dust formation region. Further inside a very steep temperature increase further is the signature of the photosphere of the star.

Figure 7 shows the relevant quantities which describe the dust formation in the wind. In Fig. 7a the nucleation rate J_ℓ and the growth velocity (da/dt) are plotted (cf. definitions in Sect. 5.3.1). Close to the star, dust formation is still in the starting phase, at least as far as the nucleation rate is concerned. However, the growth velocity of the dust grain radii is large in this region. Consequently, the particles grow to rather large sizes. This effect is further amplified by the long time the material stays at about the same place due to the small wind velocities. The total effect can be clearly seen from the mean grain radius (Fig. 7b), which peaks at a value of about 1cm. However, these very few big particles are a consequence of the assumptions of the model: *stationarity* and *effective coupling* between dust and gas. Actually, the assumption of strict grain coupling to the gas is rather poor for grains that are large and they will drift out of the inner regions of the wind before they reach such an extreme size. Furthermore, the variability of most stars on the AGB will prohibit constant growth conditions for times longer than a few years.

Around the sonic point J_ℓ is rapidly increasing. The maximum value is reached slightly outside the sonic point - so most of the nuclei are produced in this region. Also, the growth velocity decreases by an order of magnitude around the sonic point, mainly due to the rapid dilution of the wind material. Due to the large nucleation rate around the peak, many small particle are formed which do not grow as efficiently as before. A rapid drop in the mean grain radius is the result. After the peak of J_ℓ only few new particles are produced. The remaining grains grow slowly and increase the mean grain radius to its final value of about 0.1μ.

The dust grain size distribution function at four different sites in the wind is shown in Fig. 8. Again it can be seen that the very large particles are produced in the inner region of the wind. At $1.6R_0$, the large particle end of the size distribution function already has developed its final shape, since for these grains the growth process farther out in the wind contributes only a small fraction of

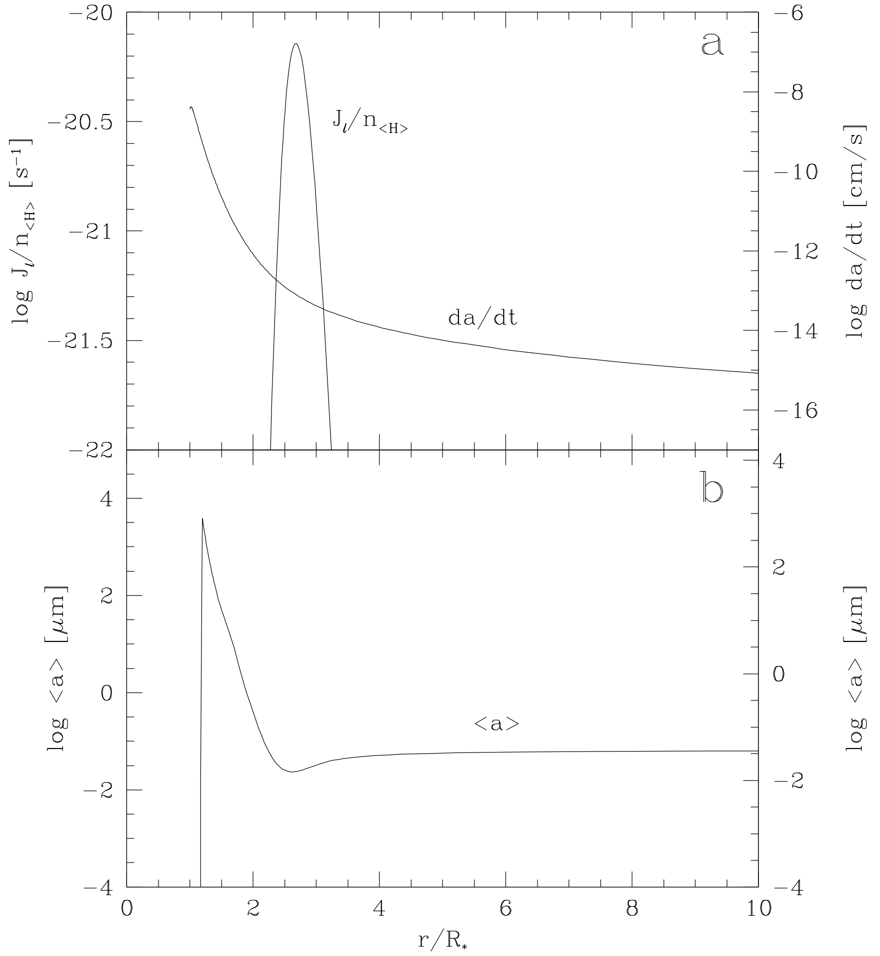

Fig. 7. The quantities describing the formation of dust. a) nucleation rate per hydrogen atom $\hat{J}_\ell$ and growth velocity of the dust grain radii da/dt. b) mean grain radius $< a >= K_1/K_0$.

the sizes they already have obtained near their nucleation point. The opposite is true for the smaller particles which are added around the sonic point. For these grains, the subsequent growth at larger distances from the star makes an important contribution to their final size.

An interesting point is that the size distribution function results to be approximately a power law for particle sizes $0.05\mu < a < 100\mu$ with an exponent β of about -4.3 (cf. Sect. 3.3.2). It can be shown that this is a typical signature of a dust driven wind ([Dominik *et al.* 1989]). The basic reason for this distribution is that in a purely dust driven wind the region of wind generation and the region of dust formation always coincide (cf. Sects. 1 and 3.2.1b). The onset of

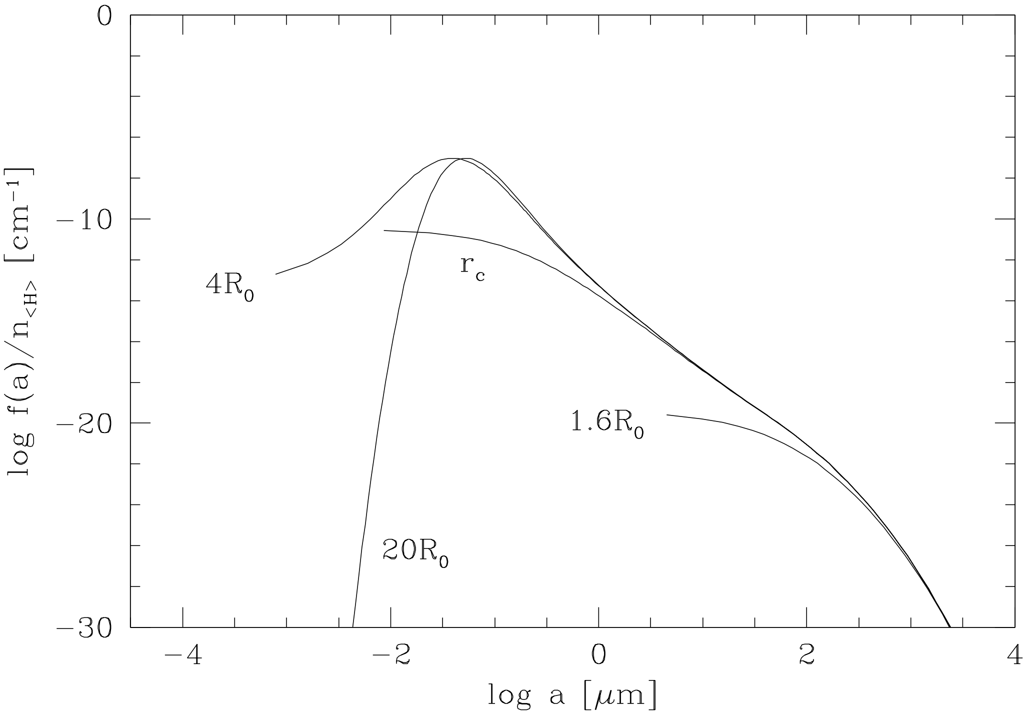

Fig. 8. The size distribution of the dust component at different positions in the envelope of the model discussed in the text.

dust formation necessarily occurs around the sonic point, where the densities and the time scales associated with the wind velocity change very rapidly. Particles produced at different places by very different nucleation rates are subject to very different growth conditions which leads to a stretched power law distribution. If the complete nucleation peak were located inside the sonic point, few very big particles would be the result. If it were located completely outside the sonic point, many but small particles would be formed.

Fig. 9 shows the emergent spectrum of the model discussed above together with observational data of the carbon star IRC+10216, taken from different authors, measured near the time of luminosity maximum (see [Winters *et al.* 1994]). The agreement is very satisfactory and shows, that important aspects of the appearance of AGB stars may in fact be explained in the frame of dust driven winds. Nevertheless it should be kept in mind that these model calculations are stationary and do not consider contributions from wave dissipation which might be important for the inner structure of the wind.

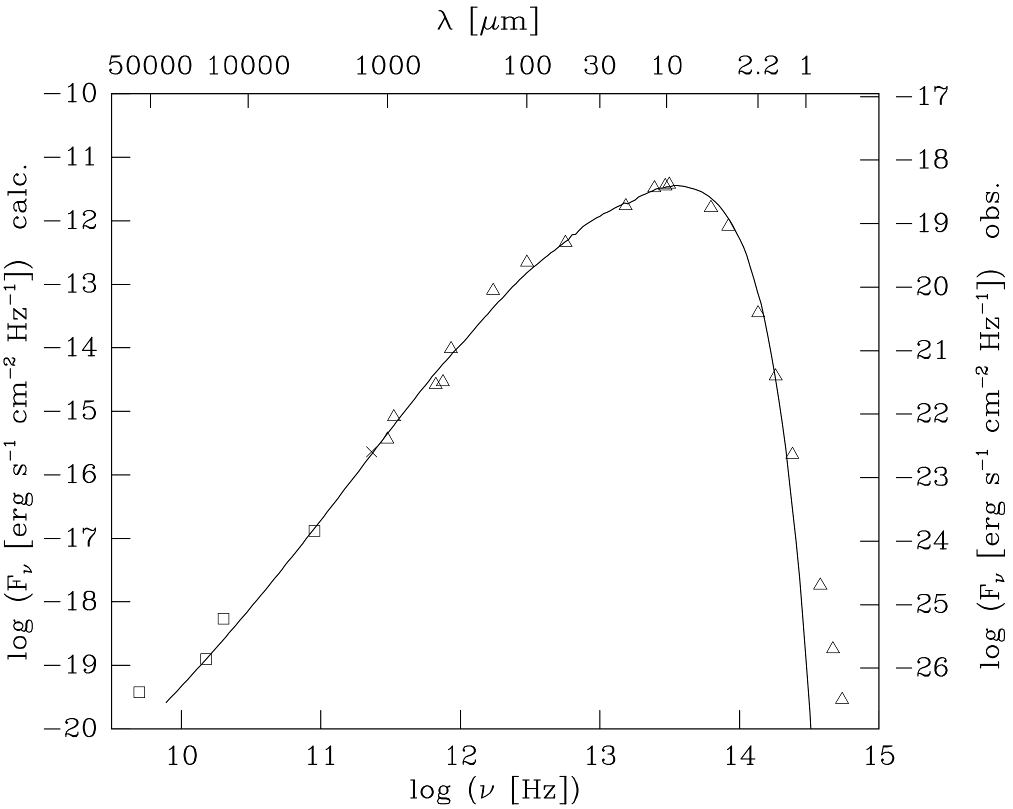

Fig. 9. The emergent spectrum of the model discussed in the text, plotted together with observed fluxes for the carbon star IRC+10216 (after [Winters *et al.* 1994]).

6.3 Dust driven mass loss

We have seen, that dust formation in a stellar wind provides an effective wind driving mechanism. Dust formation thus is a possible cause of the massive mass loss experienced by red giants on the AGB. In fact, dust driven winds can be considered as some lower limit of the mass loss mechanism since additional processes like the levitation of the atmosphere by molecular absorption and by wave dissipation certainly would also have the tendency to increase the mass loss.

In order to look at the mass loss rates produced by dust driven winds it is advantageous to treat $\dot{M}$ as a dependent quantity which has to be calculated from the model. We may then evaluate the mass loss rate in terms of the mass of the star M_*, its luminosity L_*, and its photospheric temperature T_*, and the abundance ratio $\varepsilon_C/\varepsilon_O$.

As already discussed in Sect. 3.3.2, a purely dust driven wind can only exist for a restricted set of stellar parameters. For the type of model calculations discussed in the previous section, such a parameter range study has been performed by Dominik et al. (1990). However, these models do not include the detailed treatment of radiative transfer, which was replaced by the Lucy approximation (see Appendix). The absorption properties of the dust grains were calculated under the assumption that the dust particles are small. We will discuss some of the results here.

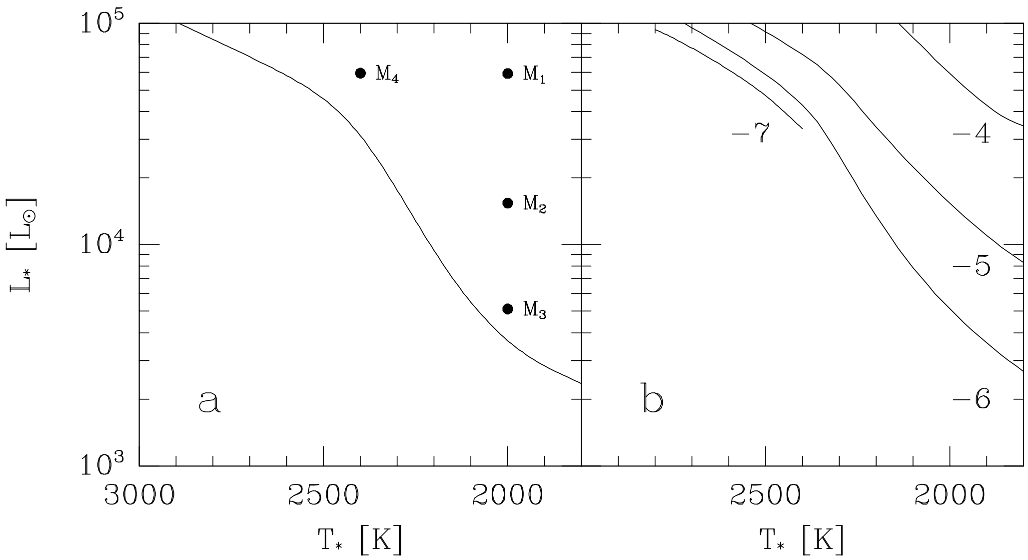

Fig. 10. HR-diagram for the dust driven winds around carbon stars with $M_* = 1M_\odot$ and $\varepsilon_C/\varepsilon_O = 2$. In the left diagram (a), the limiting line for dust driven winds is shown. The marks $M_1 \ldots M_4$ denote the positions of the four models used later on in the discussion on the dependence of the mass loss rate on M_* and $\varepsilon_C/\varepsilon_O$. The right diagram (b) shows contour lines of constant mass loss rate with logarithmic labels in units $M_\odot \mathrm{yr}^{-1}$.

A purely dust driven wind solution is possible only above a certain luminosity, which is of the order of $10^4 L_\odot$. However, the exact value depends upon the photospheric temperature of the star, its mass and upon the chemical abundances in the atmosphere. For fixed mass and abundances one may draw a line in the HR diagram which defines the Eddington limit for these stars (Fig 10a). Above this critical line, a self maintaining dust driven wind solution is possible, below it is not (cf. Sect. 3.3.2).

For fixed values of M_* and $\varepsilon_C/\varepsilon_O$, we may also plot contour lines of constant mass loss rate in the HRD (Fig. 10b). The minimum mass loss rate, at positions near the Eddington limit, is of the order of $10^{-7} M_\odot \mathrm{yr}^{-1}$. The mass loss rate is a steeply rising function of increasing luminosity and decreasing photospheric temperature. Hence, mass loss rates as high as $10^{-4} M_\odot \mathrm{yr}^{-1}$ can easily be obtained for sufficiently high values of the luminosity.

The influences of the remaining parameters $\varepsilon_C/\varepsilon_O$ and M_* can be taken from Figs. 11 and 12, respectively, for four different pairs of L_*, T_*. A very interesting

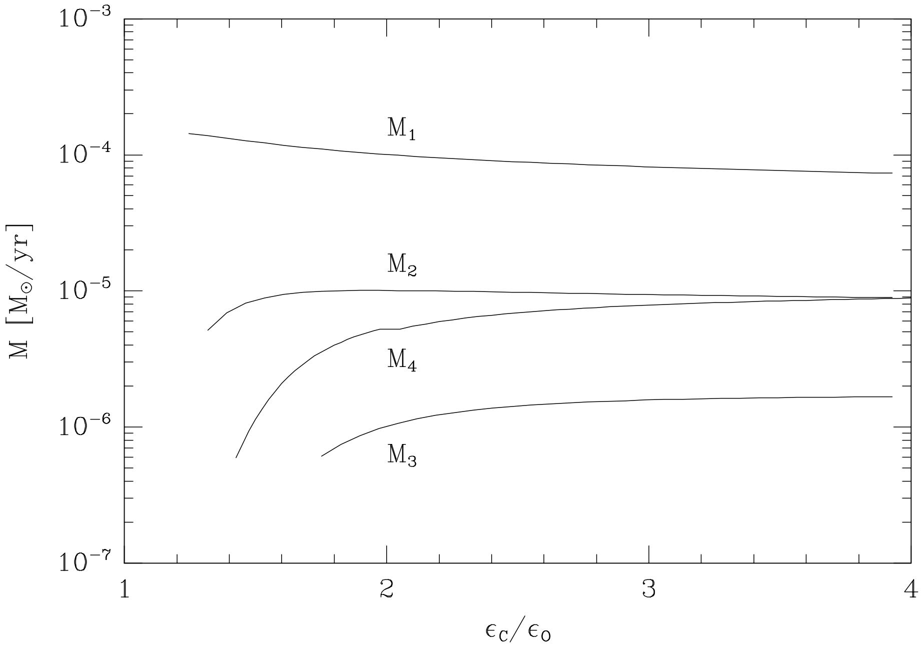

Fig. 11. Dependence of the mass loss rate on the overabundance of carbon relative to oxygen for the four models marked in Fig. 10.

point is that $\dot{M}$ shows hardly any dependence upon the abundance of the condensing material. Of course, if this abundance is to low, no purely dust driven solution does exist since dust formation itself is not possible in an effective way. However, above a critical overabundance (about $\epsilon_C/\epsilon_O \simeq 1.3$ in the considered model), the wind can be driven by the dust component. Any further enhancement of the wind material with carbon does not influence the mass loss rate but rather increases the resulting wind velocity ([Dominik *et al.* 1990]). The reason for this behaviour is, that only a certain minimum amount of dust is needed to push the wind through the sonic point, and the abundance of the condensing material only must be high enough to provide this critical acceleration. Higher abundances of condensable material will lead to further condensation *outside* the sonic point. However, since there the wind is already supersonic, no information is fed back inside the sonic point where the mass loss rate is determined (cf. Sect. 1).

The dependence of the mass loss rate upon the stellar mass M_* is shown in Fig. 12 for the same pairs of L_*, T_* as above. M_* has been varied from 0.5 $M_\odot$, which is the typical mass of white dwarfs and, therefore, a reasonable lower limit, up to the highest mass possible for a purely dust driven wind. $\dot{M}$ obviously increases dramatically with decreasing mass. A reduction of M_* by 50% may cause an increase in the mass loss rate by a factor of 3 to 100. This intuitively

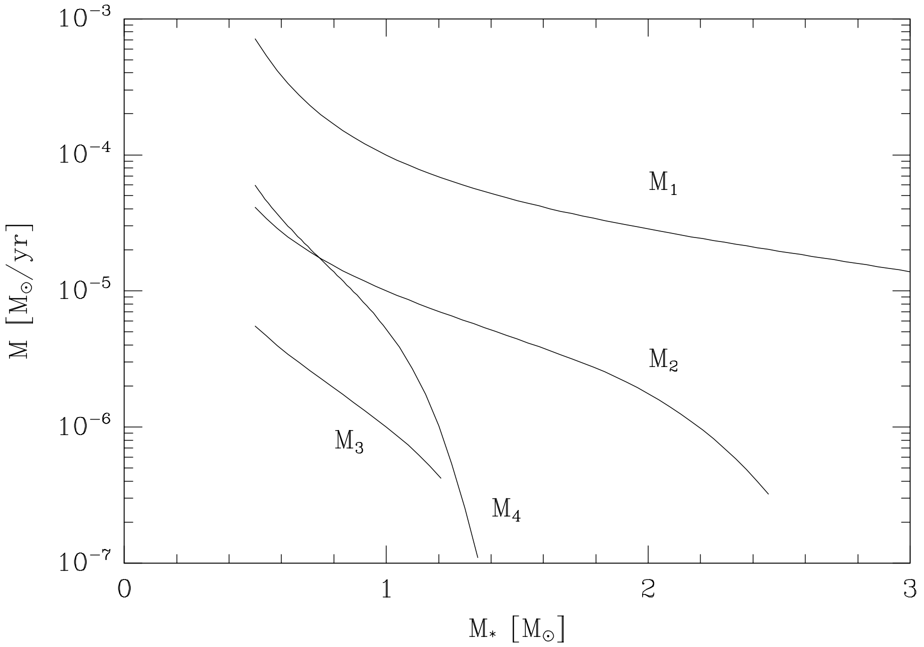

Fig. 12. Dependence of the mass loss rate on the stellar mass for the four models marked in Fig. 10.

suggests a possible mass loss instability. Once a star has reached in its evolution the limit where dust driven winds are possible, it looses mass with a time scale $M_*/\dot{M}$. This time scale is typically 10^4 to 10^7 yr and, therefore, smaller than the time scale for evolution due to nuclear burning, which on the AGB is about 10^7 yr. If we neglect for simplicity possible variations in the photospheric temperature and in the luminosity and integrate the mass loss rate over time, we get an evolution of the stellar mass, which is shown for four different stars (again the previously used L_* and T_* combinations with $\varepsilon_C/\varepsilon_O = 2$) in Fig. 13. It is obvious, that the mass loss is in fact unstable and can lead to the ejection of half a solar mass within 10^4 yr or less. This makes dust driving an attractive mechanism for the final ejection of the envelope of an AGB star and its transition to a planetary nebula, especially when we consider the cooperative effects of other mechanisms.

If we put together the different dependences of dust driven mass loss, from our models of C-stars a fit formula for $\dot{M}$ as function of the fundamental stellar parameters may be derived:

$$\dot{M} = 10^{-3.7-0.93M_*}(\log L_* - T_*/600K)^{(1.71+2.59M_*)} \qquad (6.1)$$

where M_* and L_* are measured in solar units and $\dot{M}$ in solar masses per year. These results compare reasonably well with the mass loss studies by [deJager *et*

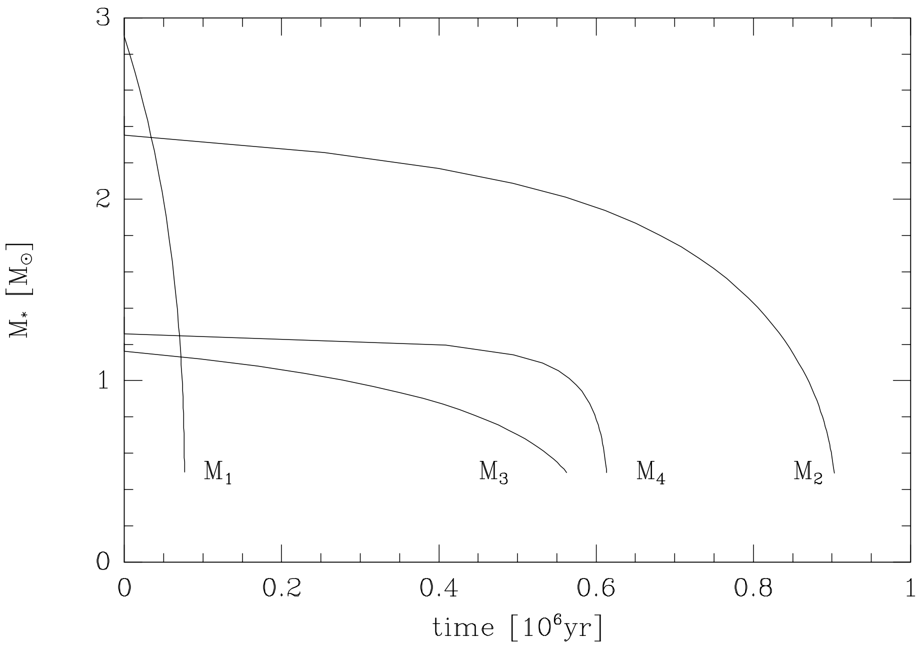

Fig. 13. Theoretical time evolution of the stellar mass with the assumption of constant L_*andT_*. These parameters are given by the marks in Fig. 10. For M_2, M_3, M_4, $t = 0$ is the onset of a dust driven wind when the star meets the dividing line for the possibility of a purely dust driven wind. M_1 has been shifted by an appropriate value in time.

al. 1988] for carbon stars on the AGB ([Dominik *et al.* 1990]).

7 Conclusions

We have surveyed the knowledge about dust driven winds around late type giant stars from a dominantly theoretical point of view. In doing so we have focused on the construction of a closed and self-consistent description of the complete physical problem of winds with radiation pressure on dust grains as its main source of energy and momentum. By now all the essential ingredients are available to make this attempt a successful one.
We have discussed in detail the various important components which are hydrodynamics, radiative transfer, chemistry, dust nucleation and growth. The phase transition between molecules and dust has been treated by the classical nucleation theory. This approach yields reasonable results for clusters not too small and convinces by its straightforward applicability, but nevertheless it has reasonable shortcomings for the molecular domain. Although some fundamental work in the dust nucleation complex remains to be done, a more realistic pathway description of carbon dust formation now seems to be in reach. An equivalent approach for

the silicate chemistry in oxygen rich environments is still lacking - a subject that is important for the extension of these studies towards M–stars.

Since the system of equations has been derived in closed form, the resulting models are dependent only upon a small set of parameters which describe the central star as a result of its evolutionary history up to the point where dust driven winds gain importance. These fundamental stellar parameters are mass, luminosity, temperature, and the element abundances in the gas near the photosphere from where the wind originates. The results obtained from the solution of the system of equations, such as structure of the envelope, amount of formed dust, emergent spectrum and not least the mass loss rate are in close agreement with the observed properties of dust-enshrouded objects. As these quantities are derived in a self–consistent way there is no need for additional model parameters. Besides the agreement with the overall properties of this class of late–type giant stars with massive winds, the application of this approach to model individual objects like IRC+10216 yields a close match between theoretical calculations and observational data.

Although most of the late type giants exhibit variability, the fact that for the considered class of objects a stationary approach still provides such satisfactory results points out that the structure of these envelopes is to a large extent the result of dust formation and subsequent acceleration by radiation pressure on dust grains. Thereby, the underlying stellar variability mainly triggers processes which are then shaped dominantly by the presence of dust. In this case stationary models can obviously provide also a reliable picture of the mean properties of basically time dependent objects.

An assumption made throughout this review is the neglect of drift motion between dust and gas. Whereas this simplification surely does not alter the overall picture of a dust driven wind, it will be of some importance for the size distribution function of the dust grains and therefore for the spectral appearance in the near–infrared wavelength region.

Finally, it should be recognized that the type of a purely dust driven wind does exist only for a rather restricted set of stellar parameters. It requires very high luminosities and quite low temperatures. There is no doubt that stars outside this domain also show substantial outflows and loose mass at considerable rates. Clearly, in these objects other mechanisms (some of which have been touched in this review) are active and make an important if not the main contribution to the wind generation. This can be the case even if dust formation is also present and provides additional acceleration to the outflowing material. In this sense, dust driven winds are to be considered as the 'tip of the iceberg', which due to their extremely large mass loss rates contribute a large fraction of the total galactic mass return from low mass stars to the interstellar medium. The intrinsic mass loss instability (cf. Sect. 6.3) makes this kind of winds also an attractive candidate for triggering the final ejection of the envelope at the tip of the AGB, just before these objects are turned into planetary nebulae.

Acknowledgements

The authors wish to thank Genia Schönberger, Isabelle Birambaux, Holger Beck, Axel J. Fleischer and Jan Martin Winters for their support during the completion of the manuscript.

Appendix

A Lucy's approximation

The basic idea of this approach to treat spherical radiative transfer in an extended stellar atmosphere ([Lucy 1971; Lucy 1976]) is to split the radiation field at each point $r > R_*$ into two contributions I_ν^+ and I_ν^- originating from the central star and the surrounding extended shell, respectively, and to assume that each contribution only depends on the distance r but is independent of μ.

Let $\vartheta_* = \arccos \mu_*$ denote the angle under which the star's surface is to be seen from distance $r \geq R_*$:

$$\mu_* = \left(1 - \left(\frac{R_*}{r}\right)^2\right)^{1/2} \quad . \tag{A.1}$$

According to the above assumptions, the local intensity $I_\nu(r,\mu)$ simply is given by

$$I_\nu(r,\mu) = \theta\,(\mu - \mu_*)\, I_\nu^+(r) + (1 - \theta\,(\mu - \mu_*))\; I_\nu^-(r) \tag{A.2}$$

with $\theta(x)$ being the Heavyside step function

$$\theta\,(x) = \begin{cases} 1 & \text{for } x > 0 \\ 0 & \text{for } x < 0 \end{cases} \quad . \tag{A.3}$$

Inserting (A.2) into the definition of the moments (3.43), (3.44) and (3.45) gives

$$J_\nu(r) = \frac{1}{2}\,(I_\nu^+ + I_\nu^-) - \frac{\mu_*}{2}\,(I_\nu^+ - I_\nu^-) \tag{A.4}$$

$$H_\nu(r) = \frac{1}{4}\,(I_\nu^+ - I_\nu^-) \cdot (1 - \mu_*^2) \tag{A.5}$$

$$P_\nu(r) = \frac{1}{3}\left[\frac{1}{2}(I_\nu^+ + I_\nu^-) - \frac{\mu_*^2}{2}\,(I_\nu^+ - I_\nu^-)\right] \quad . \tag{A.6}$$

Solving (A.4) and (A.5) for I_ν^+ and I_ν^- and inserting the result into (A.6) yields P_ν as a linear function of J_ν and H_ν

$$P_\nu = \frac{1}{3}\,J_\nu + \frac{2}{3}\,\mu_* H_\nu \quad , \tag{A.7}$$

and, thus, a natural closure condition for the system of the moment equations (3.48) and (3.49) which in this case reduces to

$$\frac{\partial H_\nu}{\partial r} + \frac{2}{r}\, H_\nu = -\kappa_\nu J_\nu + \epsilon_\nu \tag{A.8}$$

$$\frac{1}{3}\,\frac{\partial J_\nu}{\partial r} + \frac{2}{3}\,\frac{\partial}{\partial r}\,(\mu_* H_\nu) + \frac{2}{r}\,\mu_* H_\nu = -(\kappa_\nu + s_\nu)\, H_\nu \quad . \tag{A.9}$$

By specification of suitable boundary conditions, this system can easily be solved numerically for given absorption and emission coefficients.

Frequency integration of (A.8) and (A.9) yields

$$\frac{\partial H}{\partial r} + \frac{2}{r} H = -\int_0^\infty d\nu \kappa_\nu J_\nu + \int_0^\infty d\nu \epsilon_\nu \tag{A.10}$$

$$\frac{1}{3}\,\frac{\partial J}{\partial r} + \frac{2}{3}\,\frac{\partial}{\partial r}\,(\mu_* H) + \frac{2}{r}\,\mu_* H = -\int_0^\infty d\nu\,(\kappa_\nu + s_\nu) H_\nu \quad . \tag{A.11}$$

Under the assumption of radiative equilibrium, this system can be solved analytically for given flux average $\chi_H(r)$ of the extinction coefficient (3.54). Introducing (3.54), (3.56) and (A.1) into (A.11) results in

$$\frac{\partial}{\partial r}\,(J + 2H_*\mu_*) + \frac{2}{3}\cdot 2H_*\chi_H \left(\frac{R_*}{r}\right)^2 = 0 \quad . \tag{A.12}$$

By defining of an (inwards directed) optical depth variable ([Lucy 1971])

$$\frac{d\tau_L(r)}{dr} = -\chi_H \left(\frac{R_*}{r}\right)^2 \quad , \tag{A.13}$$

which measures both the extinction and the dilution effects, integration of (A.12) yields

$$J(r) = 2H_* \left(\frac{3}{2}\,\tau_L(r) - \mu_*(r)\right) + C \tag{A.14}$$

with C being the constant of integration.

As $J(r)$ is a monotonically decreasing function of r, C is determined by the boundary condition

$$\lim_{r\to\infty} J_\nu(r) = 0 \quad , \tag{A.15}$$

which applied to (A.14) gives

$$C = 2H_* \left(1 - \frac{3}{2}\,\tau_L(\infty)\right) \quad . \tag{A.16}$$

$\tau_L(\infty)$ is the value for the optical depth defined in (A.13) far away from the star which also vanishes for a sufficiently large r. Hence, the boundary condition for (A.13) results to

$$\tau_L(\infty) = \lim_{r\to\infty} \tau_L(r) = 0 \quad . \tag{A.17}$$

With this boundary condition, $\tau_L(r)$ is fully determined by (A.13).

Inserting (A.16) and (A.17) into the solution (A.14) yields the final result for the frequency integrated local mean intensity in the shell

$$J(r) = 2H_* \left(1 - \mu_*(r) + \frac{3}{2}\,\tau_L(r)\right) \quad , \tag{A.18}$$

expressed by the input of total flux H_* at $r = R_*$.

On the premises of LTE, (A.18) allows the immediate calculation of the temperature structure which according to (3.29) results to

$$T(r)^4 = \frac{1}{2}\,T_*^4 \left(1 - \mu_*(r) + \frac{3}{2}\,\tau_L(r)\right) \frac{\kappa_J}{\kappa_B} \quad . \tag{A.19}$$

As κ_J/κ_B remains bounded for $r \to \infty$, the result (A.19) shows that for extended spherical symmetric shells the temperature is a monotonically decreasing function with

$$\lim_{r\to\infty} T(r) = 0 \quad . \tag{A.20}$$

In order to be consistent with the relation (3.57), $T(r)$ has to meet the additional requirement

$$T(R_*) = T_* \tag{A.21}$$

which by (A.19) is equivalent to the condition

$$\tau_L(R_*) = \frac{2}{3}\left(2\,\frac{\kappa_B}{\kappa_J} - 1\right) \quad . \tag{A.22}$$

(A.17) and (A.22) can be conceived as two independent boundary conditions for the first order differential equation (A.13) which, therefore, is overdetermined. Thus, a consistent solution requires R_* to be an eigenvalue of the differential equation (A.13). Hence, R_* has to obey the equation

$$\int_{R_*}^{\infty} dr \chi_H \left(\frac{R_*}{r}\right)^2 = \frac{2}{3}\left(2\,\frac{\kappa_B}{\kappa_J} - 1\right) \tag{A.23}$$

which immediately follows from direct integration of (A.13) and the condition (A.22). By this equation, R_* is consistently determined for given L_* and T_*.

Particular simple equations are obtained if grey absorption is assumed. In this case

$$\kappa_J = \kappa_B \tag{A.24}$$

and, hence, the conditions (A.22) and (A.23) reduce to

$$\tau_L(R_*) = \int_{R_*}^{\infty} dr \chi_H \left(\frac{R_*}{r}\right)^2 = \frac{2}{3} \quad . \tag{A.25}$$

At the end of this section, a short remark on the Eddington factor introduced in (3.50): Frequency integration of this equation yields

$$P = f_J J \tag{A.26}$$

with $f_J(r)$ being the intensity averaged Eddington factor

$$f_J = \frac{1}{J} \int_0^\infty d\nu \, f_\nu J_\nu \quad . \tag{A.27}$$

In case of radiative equilibrium, Lucy's procedure allows an immediate calculation of $f_J(r)$ by inserting (A.7), (A.18), and (3.56) into (A.24)

$$f_J = \frac{1}{3} + \frac{1}{3} \left(\frac{R_*}{r} \right)^2 \frac{\mu_*(r)}{1 - \mu_*(r) + \frac{3}{2}\tau_L(r)} \quad . \tag{A.28}$$

f_J is a monotonically increasing function of r with the limit values

$$f_J(R_*) = \frac{1}{3} \tag{A.29}$$

describing the highly isotropic radiation field inside, and

$$\lim_{r \to \infty} f_J(r) = 1 \tag{A.30}$$

describing the strongly outwards directed radiation field outside, respectively. This behaviour indicates that for spherical shells the Eddington factor f_J shows no dramatic variation.

References

Alexander, D. R., Augason, G. C., and Johnson, H. R., 1989. An opacity-sampled treatment of water vapor. *ApJ*, **345**, 1014–1021.

Allard, F., Scholz, M., and Wehrse, R., 1992. Molecular Opacities in M–Star Atmospheres. *Rev. Mexicana Astron. Astrof.*, **23**, 203–215.

Baschek, B., Scholz, M., and Wehrse, R., 1991. The parameter R and T_{eff} in stellar models and observations. *A&A*, **246**, 374–382.

Beck, H. K. B., Gail, H.-P., Henkel, R., and Sedlmayr, E., 1992. Chemistry in circumstellar shells. I. Chromospheric radiation fields and dust formation in optically thin shells of M-giants. *A&A*, **265**, 626–642.

Benson, S., 1976. *Thermochemical Kinetics.* J. Wiley & Sons, New York, 2 edition.

Berruyer, N., 1991. Dust-driven winds. II. Are the grains the real cause of the motion. *A&A*, **249**, 181–191.

Berruyer, N. and Frisch, H., 1983. Dust-driven winds. I. A two-fluid model and its numerical solution. *A&A*, **126**, 269–277.

Bohren, C. F. and Huffman, D. R., 1983. *Absorption and Scattering of Light by Small Particles.* John Wiley & Sons, New York.

Bowen, G. H., 1988a. Dynamical modelling of long-period variable star atmospheres. *ApJ*, **329**, 299–317.

Bowen, G. H., 1988b. The mechanism of mass loss from pulsating cool stars. In Stalio, R. and Willson, L. A., editors, *Pulsation and mass loss in stars*, pages 3–25. Kluwer Academic Publisher.

Bowen, G. H., 1990. Dynamical phenomena in pulsating star atmospheres. In Buchler, J. R., editor, *The Numerical Modelling of Nonlinear Stellar Pulsations*, pages 155–171. Kluwer Academic Publishers.

Bowen, G. H. and Willson, L. A., 1991. From wind to superwind: The evolution of mass-loss rates for Mira models. *ApJ*, **375**, L53 – L56.

Carbon, D. F., 1979. Model atmospheres for intermediate- and late-type stars. *ARA&A*, **17**, 513–549.

Carbon, D. F., 1984. Line Blanketing. In Kalkofen, W., editor, *Methods in radiative transfer*, pages 395–426, Cambridge Univ. Press, Cambridge.

Cherchneff, I., Barker, J. R., and Tielens, A. G. G. M., 1991. Polycyclic aromatic hydrocarbon optical properties and contribution to the acceleration of stellar outflows. *ApJ*, **377**, 541–552.

Claussen, M. J., Kleinmann, S. G., Joyce, R. R., and Jura, M., 1987. A flux-limited sample of galactic carbon stars. *ApJS*, **65**, 385–404.

Danchi, W. C., Bester, M., Degiacomi, C. G., McCullogh, P. R., and Townes, C. H., 1990. Location and phase of dust formation in IRC +10216 indicated by 11 micron spatial interferometry. *ApJ*, **359**, L59–L63.

Danchi, W. C., Bester, M., Degiacomi, C. G., Greenhill, L. J., and Townes, C. H., 1994. Characteristics of dust shells around thirteen late–type stars. *AJ*, **in press**.

Deguchi, 1980. Grain formation in cool stellar envelopes. *ApJ*, **236**, 567–576.

deJager, C., 1983. *Mass Loss from Astronomical Objects; A Summary*, volume 6 of *Highlights of Astronomy*, pages 603–617. D.Reidel Publ.Comp.

deJager, C., Nieuwenhuijzen, H., and van der Hucht, K. A., 1988. Mass loss rates in the Hertzsprung–Russell diagram. *A&AS*, **72**, 259–289.

Dominik, C., 1992. *Formation of dust grains in the winds of cool giants.* PhD thesis, Technische Universität, Berlin, FRG.

Dominik, C., Gail, H.-P., and Sedlmayr, E., 1989. The size distribution of dust particles in a dust-driven wind. *A&A*, **223**, 227–236.

Dominik, C., Gail, H.-P., Sedlmayr, E., and Winters, J. M., 1990. HR diagrams for dust driven winds around C-stars. *A&A*, **240**, 365–375.

Dominik, C., Sedlmayr, E., and Gail, H.-P., 1993. Dust formation in stellar winds. VI. Moment equations for the formation of heterogeneous and core-mantle grains. *A&A*, **277**, 578–594.

Donn, B. and Nuth, J. A., 1985. Does nucleation theory apply to the formation of refractory circumstellar grains. *ApJ*, **288**, 187–190.

Draine, B. T. and Salpeter, E. E., 1977. Time dependent nucleation theory. *J.Chem.Phys.*, **67**, 2230–2235.
Dyck, H. M., Zuckerman, B., Leinert, C., and Beckwith, S., 1984. Near-infrared speckle interferometry of evolved stars and bipolar nebulae. *ApJ*, **287**, 801–813.
Dyck, H. M., Zuckerman, B., Howell, R. R., and Beckwith, S., 1987. Measurements of the circumstellar shell geometry in IRC +10216. *PASP*, **99**, 99–106.
Dyck, H. M., Benson, J. A., Howell, R. R., Joyce, R. R., and Leinert, C., 1991. The light curve and changes in the circumstellar envelope around IRC+10216. *AJ*, **102**, 200–207.
Dyck, H. M., Benson, J. A., Ridgway, S. T., and Dixon, D. J., 1992. The infrared angular diameter of α Orionis. *AJ*, **104**, 1982–1985.
Ekberg, U., Eriksson, K., and Gustafsson, B., 1986. Line blanketing in model atmospheres of carbon stars. *A&A*, **167**, 304–310.
Feder, J., Russell, K. C., Lothe, J., and Pound, G. M., 1966. Homogeneous nucleation and growth of droplets in vapours. *Adv. Phys.*, **15**, 111–178.
Fleischer, A. J., 1994. *Hydrodynamics and Dust Formation in the Circumstellar Shells of Miras and Long–Period Variables.* PhD thesis, Technische Universität, Berlin, FRG.
Fleischer, A. J., Gauger, A., and Sedlmayr, E., 1992. Circumstellar Dust shells around Long-period Variables. I. Dynamical models of C-stars including dust formation, growth and evaporation. *A&A*, **266**, 321–339.
Frenklach, M. and Feigelson, E. D., 1989. Formation of polycyclic aromatic hydrocarbons in circumstellar envelopes. *ApJ*, **341**, 372–384.
Gail, H.-P., 1990. Winds of late type stars. *Rev. Mod. Astron.*, **3**, 156–173.
Gail, H.-P. and Sedlmayr, E., 1984. Formation of crystalline and amorphous carbon grains. *A&A*, **132**, 163–167.
Gail, H.-P. and Sedlmayr, E., 1985. Dust formation in stellar winds. II. Carbon condensation in stationary, spherically expanding winds. *A&A*, **148**, 183–190.
Gail, H.-P. and Sedlmayr, E., 1986. The primary condensation process for dust around late M-type stars. *A&A*, **166**, 225–236.
Gail, H.-P. and Sedlmayr, E., 1987a. Dust formation in stellar winds. In Morfill, G. E. and Scholer, M., editors, *Physical Processes in Interstellar Clouds*, pages 275–303. D. Reidel Publ. Comp.
Gail, H.-P. and Sedlmayr, E., 1987b. Dust formation in stellar winds. III. Self-consistent models for dust-driven winds around C-stars. *A&A*, **171**, 197–204.
Gail, H.-P. and Sedlmayr, E., 1987c. Dust formation in stellar winds. V. The minimum mass loss rate for dust-driven winds. *A&A*, **177**, 186–192.
Gail, H.-P. and Sedlmayr, E., 1988. Dust formation in stellar winds. IV. Heteromolecular carbon grain formation and growth. *A&A*, **206**, 153–168.
Gail, H.-P., Keller, R., and Sedlmayr, E., 1984. Dust formation in stellar winds. I. A rapid computational method and application to graphite condensation. *A&A*, **133**, 320–332.
Gauger, A., Gail, H.-P., and Sedlmayr, E., 1990. Dust formation, growth and evaporation in a cool pulsating circumstellar shell. *A&A*, **235**, 345–361.
Gehrz, R. D., 1989. Sources of stardust in the galaxy. In Allamandola, L. J. and Tielens, A. G. G. M., editors, *Interstellar Dust*, pages 445–453, Kluwer Academic Publishers, Dordrecht.
Goeres, A., 1993. The formation of PAHs in C–type star environments. *Rev.Mod.Astron.*, **6**, 165–177.
Griffin, I. P., 1990. A model for the infrared and radio spectral energy distribution of IRC +10216 . *MNRAS*, **247**, 591–605.
Groenewegen, M. A. T., deJong, T., van der Bliek, N. S., Slijkhuis, S., and Willems, F. J., 1992. A flux-limited sample of galactic carbon stars. *A&A*, **253**, 150–172.
Gustafsson, B., 1989. Chemical analyses of cool stars. *ARA&A.*, **27**, 701–756.
Habing, H. J., 1990. The evolution of Red Giants to White Dwarfs, a review of the observational evidence. In Mennessier, M. O. and Omont, A., editors, *From Miras to Planetary Nebulae: Which path for stellar evolution?*, pages 16–40, Editions Frontières, Gif sur Yvette Cedex - France.
Habing, H. J., Tignon, J., and Tielens, A. G. G. M., 1994. Calculations of the Outflow Velocity

of Envelopes of Cool Giants. *A&A*, , in press.

Hale, B., 1986. Application of a scaled homogeneous nucleation rate formalism to experimental data at $T \ll T_C$. *Phys. Rev. A*, **33**(6), 4156–4163.

Hale, B., Kemper, P., and Nuth, J., 1989. Analysis of experimental nucleation data for silver and SiO using scaled nucleation theory. *J. Chem. Phys.*, **91**(7), 4314–4317.

Hartmann, L. and MacGregor, K. B., 1980. Momentum and energy deposition in late–type stellar atmospheres and winds. *ApJ*, **242**, 260–282.

Hearn, A. G., 1990. The physics of mass loss from AGB stars. In Mennessier, M. O. and Omont, A., editors, *From Miras to Planetary Nebulae: Which path for stellar evolution?*, pages 121–130, Editions Frontières, Gif sur Yvette Cedex - France.

Holzer, T. E. and MacGregor, K. B., 1985. Mass loss mechanisms for cool, low-gravity stars. In Morris, M. and Zuckerman, B., editors, *Mass Loss from red giants*, pages 229–255. D. Reidel Pub. Com.

Johnson, H., 1986. Thermal Atmospheric Models. In Johnson, H. and Querci, F., editors, *The M–Type Stars*, pages 323–371. CNRS.

Johnson, H. R., Bernat, A. P., and Krupp, B. M., 1980. Red giant model atmospheres. I. A Grid of opacity sampled models. *ApJS*, **42**, 501–522.

Jones, T. W., Ney, E. P., and Stein, W. A., 1981. Pulsations, grain condensation, and mass loss in long-period variable stars. *ApJ*, **250**, 324–326.

Jørgensen, U., 1992a. Molecular Opacity Data for Stellar Atmospheres. *Rev. Mexicana Astron. Astrofis.*, **23**, 49–62.

Jørgensen, U., 1992b. Sampling Methods. *Rev. Mexicana Astron. Astrofis.*, **23**, 195–202.

Jørgensen, U. G., editor, 1994. *IAU Colloquium 146: Molecules in the Stellar Environment* , Springer Verlag, Berlin.

Jørgensen, U. G. and Johnson, H. R., 1992. Radiative force on molecules and its possible role for mass loss in evolved AGB stars. *A&A*, **265**, 168–176.

Jørgensen, U. G., Johnson, H. R., and Nordlund, Å., 1992. Effects of sphericity in carbon star atmospheres. *A&A*, **261**, 263–273.

Jura, M., 1983. The dust around the carbon star IRC +10216. *ApJ*, **267**, 647–652.

Jura, M., 1986a. Mass loss from carbon stars. *ApJ*, **303**, 327–332.

Jura, M., 1986b. The Role of dust in mass loss from late-type stars. *Irish astr. J.*, **17**, 322–330.

Jura, M. and Kleinmann, S. G., 1989. Dust–enshrouded asymptotic giant branch stars in the solar neighborhood. *ApJ*, **341**, 359–366.

Jura, M., Joyce, R. R., and Kleinmann, S. G., 1989. High–luminosity carbon stars in the galactic anticenter. *ApJ*, **336**, 924–936.

Keller, R., 1987. Polyaromatic hydrocarbons and the condensation of carbon in stellar winds. In Léger, A., d'Hendecourt, L., and Boccara, N., editors, *Polycyclic Aromatic Hydrocarbons and Astrophysics*, pages 387–397. Reidel Publ. Comp.

Kerker, M., 1969. *The scattering of light.* Academic Press, New York–London.

Knapp, G. R., 1985. Mass Loss from evolved stars. IV. The dust-to-gas ratio in the envelopes of Mira variables and carbon stars. *ApJ*, **293**, 273–280.

Knapp, G. R., 1986. Mass loss from evolved stars. VI. Mass-loss mechanisms and luminosity evolution. *ApJ*, **311**, 731–741.

Knapp, G. R., 1987. Mass loss from carbon stars – Observations of the CO millimeter wavelength rotational lines. In Kwok, S. and Pottasch, S. R., editors, *Late Stages of Stellar Evolution*, pages 103–118, D. Reidel Publishing Company, Dordrecht, Holland.

Knapp, G. R. and Morris, M., 1985. Mass loss from evolved stars. III. Mass loss rates for 50 Stars from CO $J = 1 - 0$ observations. *ApJ*, **292**, 640–669.

Knapp, G. R., Phillips, T. G., Leighton, R. B., Lo, K. Y., Wannier, P. G., Wooten, H. A., and Huggins, P., 1982. Mass Loss from evolved stars. I. Observations of 17 stars in the CO $(2-1)$ line. *ApJ*, **252**, 616–634.

Kozasa, T. and Hasegawa, H., 1987. Grain Formation through Nucleation Process in Astrophysical Environments. II. *Prog.Theor.Phys.*, , 1402–1410.

Kozasa, T., Hasegawa, H., and Seki, J., 1984. Grain formation in the expanding gas flow around cool luminous stars. *Ap&SS*, **98**, 61–79.

Kudritzki, R., Gabler, R., Kunze, D., Pauldrach, A., and Puls, J., 1991. Model Atmospheres of Hot Stars. In Leitherer, C., Walborn, N., Heckman, T., and Norman, C., editors, *Massive Stars in Starbursts*, pages 59–96, Cambridge University Press, Cambridge.

Kurucz, R., 1994. Computation of Opacities for Diatomic Molecules. In Jørgensen, U. G., editor, *IAU Colloquium 146: Molecules in the Stellar Environment*, pages 282–295, Springer–Verlag, Berlin.

Kwok, S., 1975. Radiation pressure on grains as a mechanism for mass loss in red giants. *ApJ*, **198**, 583–591.

Lafon, J.-P. and Berruyer, N., 1991. Mass loss mechanisms in evolved stars. *A&AR*, **2**, 249–289.

LeBertre, T., 1987. The opacity of the dust around the carbon star IRC + 10216. *A&A*, **176**, 107–113.

LeBertre, T., 1988a. Optical and infrared observations of IRC+10216 and related objects. Dust shells modelling. *A&A*, **203**, 85–98.

LeBertre, T., 1988b. Optical and infrared observations of the carbon Mira R For. Dust shell modelling as a function of phase. *A&A*, **190**, 79–86.

Loup, C., Forveille, T., Omont, A., and Paul, J. F., 1993. CO and HCN observations of circumstellar envelopes. A catalogue – mass loss rates and distributions. *A&AS*, **99**, 291–377.

Lucy, L. B., 1971. The formation of resonance lines in extended atmospheres. *ApJ*, **163**, 95–110.

Lucy, L. B., 1976. Mass loss by cool carbon stars. *ApJ*, **205**, 482–491.

Lynas-Gray, A. E., Mendoza, C., and Zeippen, C. J., editors, 1992. *Circumstellar envelopes and mass loss of red giants. Workshop on astrophysical opacities.*, Revista Mexicana de Astronomia y astrofisica, Vol. 23, Caracas, Venezuela.

MacGregor, K. B. and Stencel, R. E., 1992. On the interaction between dust and gas in late-type stellar atmospheres and winds. *ApJ*, **397**, 644–651.

Mamon, G. A., Glassgold, A. E., and Huggins, P. J., 1988. The photodissociation of CO in circumstellar envelopes. *ApJ*, **328**, 797–808.

Maron, M., 1990. Optical properties of fine amorphous carbon grains in the infrared region. *Ap&SS*, **172**, 21–28.

Martin, P. G. and Rogers, C., 1987. Carbon grains in the envelope of IRC +10216. *ApJ*, **322**, 374–392.

McCarthy, D. W., Howell, R., and Low, F. J., 1980. Spatial spectra of IRC +10216 from 2.2 to 20 microns. Deviations from spherical symmetry. *ApJ*, **235**, L27–L31.

Menietti, J. D. and Fix, J. D., 1978. Models of mass flows from cool, luminous stars. *ApJ*, **224**, 961–968.

Olofsson, H., Eriksson, K., Gustafsson, B., and Carlström, U., 1993a. A study of circumstellar envelopes around bright carbon stars. I. Structure, kinematics, and mass loss rate. *ApJS*, **87**, 267–304.

Olofsson, H., Eriksson, K., Gustafsson, B., and Carlström, U., 1993b. A study of circumstellar envelopes around bright carbon stars. II. Molecular abundances. *ApJS*, **87**, 305–330.

Orofino, V., Colangeli, L., Bussoletti, E., Blanco, A., and Fonti, S., 1990. Amorphous carbon grains and emission spectra of IRC+10216. *A&A*, **231**, 105–110.

Pijpers, F. P. and Habing, H. J., 1989. Driving the stellar wind of AGB stars by acoustic waves; exploration of a simple model. *A&A*, **215**, 334–346.

Pijpers, F. P. and Hearn, A. G., 1989. A model for the stellar wind driven by linear acoustic waves. *A&A*, **209**, 198–210.

Plez, B., Brett, J. M., and Nordlund, A., 1992. Spherical opacity sampling model atmospheres for M giants I. Techniques, data and discussion. *A&A*, **256**, 551–571.

Querci, F., Querci, M., and Tsuji, T., 1974. Model atmospheres for C type stars. *A&A*, **31**, 265–282.

Rawlings, J. M. C. and Williams, D. A., 1989. Chemical routes to dust formation in the ejecta of novae. *Mon.Not.R.astr.Soc.*, **240**, 729–740.

Reimers, D., 1975. Circumstellar envelopes and mass loss of red giants. In Baschek, B., Kegel, W. H., and Traving, G., editors, *Problems in stellar atmospheres and envelopes*, pages 229–256, Springer Verlag, Berlin–Heidelberg.

Ridgway, S. T. and Keady, J. J., 1988. The IRC +10216 circumstellar envelope. II. Spatial

measurements of the dust. *ApJ*, **326**, 843–858.
Ridgway, S. T., Joyce, R. R., Connors, D., Pipher, J. L., and Dainty, C., 1986. The dust shells of NML Cygnus and IRC 10420: Inner radius, temperature, and optical thickness. *ApJ*, **302**, 662–674.
Rose, W. K., 1987. Infrared continuum radiation from red giants. *ApJ*, **312**, 284–289.
Salpeter, E. E., 1974a. Formation and flow of dust grains in cool stellar atmospheres. *ApJ*, **193**, 585–592.
Salpeter, E. E., 1974b. Nucleation and growth of dust grains. *ApJ*, **193**, 579–584.
Salpeter, E. E., 1977. Formation and destruction of dust grains. *ARA&A*, **15**, 267–293.
Sedlmayr, E., 1994. From molecules to grains. In Jørgensen, U. G., editor, *IAU Colloquium 146: Molecules in the Stellar Environment*, pages 163–185, Springer–Verlag, Berlin.
Sedlmayr, E. and Winters, J. M., 1991. Dust in the shells of cool giants and supergiants. In Crivellari, L., Hubeny, I., and Hummer, D. G., editors, *Stellar Atmospheres: Beyond Classical Models*, pages 397–408. Kluwer Academic Publishers.
Sopka, R. J., Hildebrand, R., Jaffe, D. T., Gatley, I., Roelling, T., Werner, M., Jura, M., and Zuckerman, B., 1985. Submillimeter observations of evolved stars. *ApJ*, **294**, 242–255.
Sopka, R. J., Olofsson, H., Johansson, L. E. B., Nguyen-Q-Rieu, and Zuckerman, B., 1989. Molecular emission lines from the envelopes of evolved stars. *A&A*, **210**, 78–92.
Sutton, E. C., Storey, J. W. V., Betz, A. L., Townes, C. H., and Spears, D. L., 1977. Spatial heterodyne interferometry of VV Canis Majoris, Alpha Orionis, Alpha Scorpii, and R Leonis at 11 microns. *ApJ*, **217**, L97–L100.
Sutton, E. C., Storey, J. W. V., Townes, C. H., and Spears, D. L., 1978. Variations in the spatial distribution of 11 micron radiation from Omicron Ceti. *ApJ*, **224**, L123–L126.
Sutton, E. C., Betz, A. L., Storey, J. W. V., and Spears, D. L., 1979. The brightness distribution of IRC +10216 at 11 microns. *ApJ*, **230**, L105–L108.
Thronson, H. A., Latter, W. B., Black, J. H., Bally, J., and Hacking, P., 1987. Properties of evolved mass–losing stars in the Milky Way and variations in the interstellar dust composition. *ApJ*, **322**, 770–786.
Tielens, A., 1983. Stationary flows in the circumstellar envelopes of M giants. *ApJ*, **271**, 702–716.
Tsuji, T., 1986. Molecules in stars. *ARA&A*, **24**, 89–125.
van der Veen, W. E. C. J. and Rugers, M., 1989. A comparison between CO-, OH- and IR-mass-loss rates of evolved stars. *A&A*, **226**, 183–202.
Wickramasinghe, N. C., Donn, B. D., and Stecher, T. P., 1966. A mechanism for mass ejection in red giants. *ApJ*, **146**, 590–593.
Willems, F. J. and de Jong, T., 1988. IRAS low resolution spectra of cool carbon stars. IV. A scenario for carbon star evolution. *A&A*, **196**, 173–184.
Winters, J. M., 1994. *Internal structure and optical appearance of circumstellar dust shells around cool carbon giants*. PhD thesis, Technische Universität, Berlin, FRG.
Winters, J. M., Fleischer, A. J., Gauger, A., and Sedlmayr, E., 1993. Circumstellar Dust shells around Long-period Variables. II. Theoretical lightcurves of C–stars. *A&A*, **submitted**.
Winters, J. M., Dominik, C., and Sedlmayr, E., 1994. Theoretical spectra of circumstellar dust shells around carbon-rich asymptotic giant branch stars. *A&A*, **in press**.
Yamamoto, T. and Hasegawa, H., 1977. Grain formation through nucleation process in astrophysical environment. *Prog. Theor. Phys.*, **58**(3), 816–828.
Zuckerman, B. and Dyck, H. M., 1986. Carbon Monoxide Emission from Stars in the IRAS and Revised AFGL Catalogs. I. Mass Loss driven by Radiation pressure on Dust grains. *ApJ*, **304**, 394–400.